Palaeontology
The Palaeontological Association
www.palass.org
[Palaeontology, Vol. 69, Part 2, 2026, e70057]

The early origin of Iguanodontia: new insights into the macroevolution, diversity and biogeography of the clade

by FILIPPO MARIA ROTATORI[1,2,†*], ALFIO ALESSANDRO CHIARENZA[3,†*], FEDERICO FANTI[4] *and* MIGUEL MORENO-AZANZA[1,2,5]

[1]GEOBIOTEC, Department of Earth Sciences, NOVA School of Science and Technology, Universidade NOVA de Lisboa, P-2829 516 Campus de Caparica, Caparica, Portugal; f.rotatori@campus.fct.unl.pt, filippo.rotatori.93@gmail.com
[2]Museu da Lourinhã, Rua João Luis de Moura 95, 2530-158 Lourinhã, Portugal
[3]Department of Earth Sciences, University College London, Gower Street, London WC1E 6BT, UK; alfio.chiarenza@ucl.ac.uk, a.chiarenza15@gmail.com
[4]Dipartimento di Scienze Biologiche, Geologiche e Ambientali, Alma Mater Studiorum, Universita di Bologna, Via Zamboni 67, Bologna 40126, Italy
[5]Aragosaurus-IUCA, Recursos Geológicos y Paleoambientes, Facultad de Ciencias, Universidad de Zaragoza, 50009 Zaragoza, Spain
*Corresponding author

Typescript received 1 August 2025; accepted in revised form 19 March 2026

Abstract: Iguanodontia (Dinosauria, Ornithischia) is a speciose group of herbivorous dinosaurs that include the famous genus *Iguanodon*, one of foundational members of the clade Dinosauria. Despite their very long history of research, several aspects of their systematic relationships and their evolutionary history remain somewhat nebulous. There is currently a lack of consensus between different phylogenetic matrices due mainly to: (1) undersampling of postcranial characters; and (2) the absence of several key taxa. We assembled a data matrix from pre-existing datasets, integrating our observations on several overlooked species (mainly from Europe) and extensively sampling cranial and postcranial characters, thereby creating one of the most complete datasets for iguanodontian dinosaurs to date. We performed a series of phylogenetic analyses, employing maximum parsimony and Bayesian inference, and an historical biogeographic analysis. Overall congruent topologies between the two methods recovered, for the first time, a new clade of high-sailed styracosternans here named Ouranosauria. We ran different Bayesian inference analyses, employing morphoclock and fossilized birth–death models. Some of the tip-dated analyses, indicated an Early to Middle Jurassic origin of Iguanodontia during a palaeoclimatically (hyperthermal) and palaeogeographically (continental fragmentation) dynamic context. According to this scenario, the Iguanodontian major radiation could be tracked back to the Pliensbachian–Toarcian, pre-dating by 16 million years the first ichnological evidence attributed to this clade. Furthermore, the diversification of all the major clades occurred by the Late Jurassic, then experienced local extinction events in different areas during the Early Cretaceous. Prior to the Jurassic–Cretaceous transition, iguanodontians spread globally.

Key words: Dinosauria, phylogenetics, Jurassic, Cretaceous, systematics, Iguanodontia.

IGUANODONTIA (*sensu* Madzia *et al.* 2021) is a dinosaur clade that includes *Iguanodon*, one of the foundational members in the earliest definition of Dinosauria (Owen 1842), and one of the most speciose groups of ornithischian dinosaurs (Norman 2004). Iguanodontians are known from all continents, and have a very long history of research (Horner *et al.* 2004; Norman 2004; Dieudonné *et al.* 2020). The oldest representatives of this clade are known from the Middle–Upper Jurassic of Europe (Ruiz-Omeñaca *et al.* 2006) and ichnological evidence supports them already being present in Europe and North Africa as early as the Bathonian (dePolo *et al.* 2020; Klein *et al.* 2023; Oussou *et al.* 2023). During the Late Jurassic, iguanodontians represented a minor component of global faunal assemblages (Foster 2020), while herbivorous dinosaurs were mainly represented by sauropodomorphs and thyreophorans. Early Cretaceous faunas show a reversed situation, where iguanodontians achieved global distribution and are the most abundant herbivorous dinosaurs, with subordinate abundances of sauropods and thyreophorans (Galton 2009; Chiarenza *et al.* 2022). This large-scale trophic turnover occurred between the Late Jurassic and the lower half (pre-Barremian) of the Early Cretaceous, although the abruptness of this event is still a matter of debate. The fossil record of both the USA (Utah) and the UK suggests that the Jurassic–Cretaceous turnover was abrupt (Edgar *et al.* 2023; Kirkland

†These authors equally contributed to this work.

doi: 10.1111/pala.70057

et al. 2025), whereas the Angéac-Charente Fossil-Lagerstätte in France (the only site firmly dated to the Berriasian) shows no significant difference in palaeodiversity and faunal composition from Late Jurassic ecosystems (Allain *et al.* 2022).

Systematic inter-relationships of the earlier diverging iguanodontian forms (i.e. non-hadrosaurids) and their macroevolutionary history have been subject of debates regarding especially the affinities of some of the earliest taxa and what the ingroup Iguanodontia includes (McDonald 2012; Verdú *et al.* 2015; Bell *et al.* 2018; Xu *et al.* 2018; Cruzado-Caballero *et al.* 2019; Herne *et al.* 2019; Rozadilla *et al.* 2019; Dieudonné *et al.* 2020; Poole 2022; Alarcón-Muñoz *et al.* 2023). Specifically, recent time calibrated phylogenetic analyses focusing on the inter-relationships of the early diverging ornithischians pushed back the origin of Iguanodontia to the early Middle Jurassic (Boyd 2015; Dieudonné *et al.* 2020; Poole 2022), with some analyses suggesting an even earlier origin (Rotatori et al. 2023; Panciroli *et al.* 2025). These recent finds imply a long ghost lineage, which hampers our understanding of early diversification patterns within this clade during the earliest stages of the Jurassic. Moreover, divergence times for the main clades appearing in the fossil record in the Lower Cretaceous (e.g. Iguanodontidae, Hadrosauroidea) seem to be inconsistent between different analyses (Boyd 2015; Dieudonné *et al.* 2020; Poole 2022). The main disagreements among the topologies recovered and their implied macroevolutionary histories are due to uneven taxon sampling within matrices and over-representation of cranial characters in the datasets, as has been shown in the case of earlier diverging neornithischians (McDonald 2012; Boyd 2015; Xu *et al.* 2018; Brown *et al.* 2021). In many of the above-mentioned analyses, the growing European fossil record of iguanodontians dated to the Late Jurassic and Early Cretaceous is key, although currently underrepresented, obscuring this major transition in the macroevolution of Iguanodontia and the potential implications on understanding the biogeography of the earlier diverging, European forms of this clade.

For this contribution, we compiled a novel dataset that includes several Late Jurassic and Early Cretaceous European iguanodontians combining a reappraisal of historical specimens and new discoveries (Ruiz-Omeñaca 2011; Escaso *et al.* 2014; Verdú *et al.* 2015; Vidarte *et al.* 2016; Maidment *et al.* 2022; Rotatori *et al.* 2022, 2025; Bonsor *et al.* 2023; Sánchez-Fenollosa *et al.* 2023). We made an effort to thoroughly sample the usually overlooked postcranial skeletons, by means of compiling characters from pre-existing datasets, in order to build a more balanced dataset for different anatomical districts. The topology resulting from phylogenetic analyses was then analysed to explore the evolutionary and biogeographical history of the clade Iguanodontia.

MATERIAL & METHOD

Taxon sampling

The current data matrix includes most non-hadrosaurid iguanodontian species known in the fossil record, focusing specifically on non-hadrosauroid iguanodontians. Furthermore, we reviewed and included several neglected specimens from the Late Jurassic and Early Cretaceous of Europe. We used the dataset of Xu *et al.* (2018) as a starting point, implementing subsequent modifications from the literature (Lockwood *et al.* 2021; Rotatori *et al.* 2022) and novel additions based on our own observations. A preliminary version of this dataset was recently published (Rotatori *et al.* 2025). We preferred the above-mentioned dataset as a starting point, over more recent ones (i.e. Poole 2022) for the following reasons: Xu *et al.* (2018) dataset has been frequently updated and revised by several specialists (i.e. Lockwood *et al.* 2021, 2024; Maidment *et al.* 2022; Rotatori *et al.* 2022, 2025; Bonsor *et al.* 2023), therefore we assume it is less prone to errors in character scoring and better reflects the current consensus. Furthermore, the results of those analyses have been considered the 'standard' for iguanodontian systematics and taxonomy for the last eight years, and therefore offer the perfect background for comparative analytical works.

For this study, we personally examined several key specimens (Table 1). Remaining specimens were scored from the available literature, integrating novel anatomical data from reappraisal of several key specimens (i.e. Chiarenza *et al.* 2021; Maidment *et al.* 2022; Bonsor *et al.* 2023). The scorings of the taxa were maintained as in the original matrices. During the expansion of the character list, we added any missing character entries to the original dataset based on a review of the literature. The only taxon that has been re-scored from its original coding is *Tethyshadros insularis*, based on first-hand observations of AAC and FF following the new published revision of this taxon (Chiarenza *et al.* 2021). The newly added taxa were mostly scored from scratch, although if present, original taxa scorings were taken into account or integrated. Newly added taxa and specimens include the following:

Iani smithi Zanno *et al.* 2023 is an early diverging-rhabdodontomorph recovered from the Cenomanian age Mussentuchit Member of the Cedar Mountain Formation, central Utah, USA (Tucker *et al.* 2023). This species represents one of the earliest known rhabdodontomorphs to date. Until the discovery of *Iani smithi*, the only well-established clade within Rhabdodontomorpha was Rhabdodontidae, that inhabited Late Cretaceous ecosystems of Europe but there was no consensus regarding which were their closer relatives (Maidment *et al.* 2026).

TABLE 1. List of the specimens examined for this study.

Taxa	Specimens
Barilium dawsoni	NHMUK R798, R798b, R799, R800–806, 4771, R4772, R4742, R2357, R3788
Camptosaurus dispar	YPM 1880, 1887; USNM 4282, 5473, 5818, 5819
Cumnoria prestwichii	OUMNH J.3303
Delapparentia turolensis	MPT/I.G.
Dryosaurus sp.	AMNH 834; CM 3392; YPM 1876
Dysalotosaurus lettowvorbecki	GPIT/RE/3612, 72385, 69069, 69068, 69064, 72408, 69075, 72333; NHMUK R6861, R8351, R12317, R12328; SMNS 52349
Hypselospinus fittoni	NHMUK R1635, R1635, R1635, R1148, R1148
Iguanodon bernissartensis	RBINS 05144, 01733
Iguanodon galvensis	MAP-4787, 4902, 5152
Magnamanus soriaensis	MNS 2000, 2001, 2002, 2003
Mantellisaurus atherfieldensis	NHMUK R11521
Proa valdeorrinaensis	MAP AR-1-2012, AR-1/19, AR-1-2013, AR-1-4413, AR-1-4439, AR-1-4370
Tenontosaurus tilletti	AMNH FARB 3061, AMNH 3040, 3039, 3014; YPM 5456
Theiophytallia kerri	YPM 1858
Uteodon aphanoecetes	CM 11337
Valdosaurus canaliculatus	IWCMS.2001.4.m, IWCMS.2013.175

Poole (2022) recovered *Tenontosaurus tilletti* as the earliest diverging member of Rhabdodontomorpha, and the anatomical characters of *Iani smithi* supported this interpretation, also in subsequent phylogenetic analyses (Fonseca *et al.* 2024). This specimen was scored by literature revision, including the scoring of its original description (Zanno *et al.* 2023).

Eousdryosaurus nanohallucis Escaso *et al.* 2014 is a species of early diverging iguanodontian dinosaur, represented so far only by the holotype SHN.JJS.170. This specimen has been dated to the uppermost Kimmeridgian beds of the Lusitanian Basin, Portugal. Escaso *et al.* (2014) recovered this taxon within Dryosauridae alongside *Dryosaurus altus*, *Dysalotosaurus lettowvorbecki*, *Valdosaurus canaliculatus*, *Kangnasaurus coetzei*, *Callovosaurus leedsi* and *Elrhazosaurus nigeriensis*. Subsequently, Dieudonné *et al.* (2020) recovered *Eousdryosaurus nanohallucis* as the earliest diverging member of Elasmaria. Later analysis, which included first hand examination of the holotype of SHN.JJS.170, recovered *Eousdryosaurus nanohallucis* within Dryosauridae (Rotatori *et al.* 2023). This interpretation was supported by other authors as well (Fonseca *et al.* 2024). This taxon was scored by first-hand examination.

Draconyx loureiroi Mateus & Antunes 2001 is represented by the holotype and sole specimen ML 357, which includes postcranial and dental material described by Mateus & Antunes (2001) and in more detail by Rotatori *et al.* (2022). This specimen was recovered from the lowermost Tithonian beds of the Lusitanian Basin, Portugal. It was originally described as a member of Camptosauridae (Mateus & Antunes 2001), but subsequently recovered as an early diverging member of Styracosterna (Rotatori *et al.* 2022, 2025). Other analyses recovered this specimen either as sister to Ankylopollexia or to *Oblitosaurus bunnueli* (Rotatori *et al.* 2023; Sánchez-Fenollosa *et al.* 2023). This specimen was scored by first hand examination.

Cumnoria prestwichii (Hulke) Seeley 1888a is based on the holotype and only specimen OUMNH J.3303, recovered from the upper Kimmeridgian beds of the Kimmeridge Clay Formation, UK. This specimen is represented by a partial skeleton that includes cranial and postcranial material (Maidment *et al.* 2022). Despite being described in the late 19th and 20th centuries (Hulke 1880; Galton & Powell 1980), this specimen was considered by some authors for a long time within the genus *Camptosaurus* (Galton & Powell 1980; Carpenter & Lamanna 2015; Carpenter & Galton 2018; Sánchez-Fenollosa *et al.* 2023), while others considered it to be a distinct genus (Seeley 1888a; McDonald 2011; Maidment *et al.* 2022; Rotatori *et al.* 2025). Since *Cumnoria* represents one of the most complete iguanodontian dinosaurs from Europe dated to the Late Jurassic, the establishment of its systematic affinities is pivotal for elucidating the early evolution of the clade. The scoring of this specimen by Maidment *et al.* (2022) was included, plus new first hand observations of additional characters not present in matrix of Xu *et al.* (2018).

Oblitosaurus bunnueli Sánchez-Fenollosa *et al.* 2023 is one of the largest sized ankylopollexian dinosaurs recovered from the Upper Jurassic of the Iberian Peninsula. It was discovered in the Kimmeridgian–Tithonian Villar del Arzobispo Fm., and is represented mainly by dental and postcranial material. It was recovered as sister to *Draconyx loureiroi* in its original description (Sánchez-Fenollosa *et al.* 2023). The authors hypothesized the presence of an Iberian Late Jurassic clade, whose recovery would have several implications regarding the evolution of this clade in Iberia. The scoring of this taxon was integrated from its original description (Sánchez-Fenollosa *et al.* 2023), with characters not present in the original of Xu *et al.* (2018) dataset scored by literature review.

SHN.JJS.015 (Ankylopollexia indet.) was described by Rotatori *et al.* (2025) and represents a new species, not

yet formally named, of large sized ankylopollexian dinosaur in the Upper Jurassic beds of the Lusitanian Basin of Portugal. Its large size is comparable with that of *Oblitosaurus bunnueli* (Rotatori *et al.* 2025), clearly differing from other coeval species. Hereafter, we refer to this specimen as 'SHN specimen' for the sake of simplicity. This specimen was scored by first hand examination.

Morelladon beltrani Gasulla *et al.* 2015 is a species of high-sailed styracosternan iguanodontian, based on the holotype and only specimen CMP-MS-03. *Morelladon* comes from Arcillas das Morellas Fm., and is Barremian in age. Gasulla *et al.* (2015) recovered this species as a styracosternan of uncertain affinities in their analysis, whereas subsequent analyses recovered as sister to *Mantellisaurus atherfieldensis* (Verdú *et al.* 2017a). This specimen was scored from the original descriptions.

Delapparentia turolensis, Ruiz-Omeñaca 2011 is represented by a very fragmentary, probably very old individual, the holotype MPT/I.G., that includes elements of pectoral and pelvic girdles, and part of the axial skeleton (Ruiz-Omeñaca 2011; Gasca *et al.* 2015). This specimen was recovered from the Camarillas Fm., dated to the lower Barremian (Medrano-Aguado *et al.* 2023). Since its formal description, the validity of this taxon has been questioned and it is often considered to be a junior synonym of *Iguanodon bernissartensis* (Verdú *et al.* 2017a; Gasulla *et al.* 2022). However, we revaluate it as a different terminal taxon than *Iguanodon bernissartensis* due to the results presented here. This specimen was scored by first hand examination.

'*Iguanodon*' *galvensis* Verdú *et al.* 2015 is based on several individuals, representing different ontogenetic stages (Verdú *et al.* 2015), recovered from the lower Barremian Camarillas Fm. (Verdú *et al.* 2015; Medrano-Aguado *et al.* 2023). This taxon has been considered the second valid species within the genus *Iguanodon* (Verdú *et al.* 2017a, 2017b). However, because it is recovered herein as more closely related to other Iberian taxa than to *Iguanodon bernissartensis*, we regard its assignment to this genus as dubious. This specimen was scored by first hand examination.

Magnamanus soriaensis, Vidarte *et al.* 2016 is an extremely robust species of styracosternan dinosaur, recovered from the uppermost Hauterivian to lower Barremian Golmayo Fm. (Vidarte *et al.* 2016). The only specimen is the holotype, an associated skeleton including cranial, axial and appendicular elements, that was previously recovered as a styracosternan of uncertain affinity (Vidarte *et al.* 2016; Santos-Cubedo *et al.* 2021). This specimen was scored by first hand examination.

The resulting matrix comprises a total of 51 terminal taxa. *Lesothosaurus diagnosticus* was set as the outgroup in all the phylogenetic analyses and the cerapodan *Hypsilophodon foxii* is the only other non-iguanodontian included. Although the non-iguanodontian cerapodan sampling may appear scarce, we note that *Hypsilophodon foxii* is the best described and documented in phylogenetic analyses among early diverging taxa, most of which have recently been considered *nomina dubia* (Barrett & Maidment 2025).

Character sampling

The original matrix (Xu *et al.* 2018) and subsequent iterations (Maidment *et al.* 2022; Bonsor *et al.* 2023) suffered from the lack of postcranial characters. In those matrices, cranial characters accounted for approximately 61% of the total, postcranial for approximately 39%. This problem was partially emended in an earlier version of the current dataset (Rotatori *et al.* 2025), although we present here the natural follow-up of that preliminary work. It is clear that both cranial and postcranial characters yield significant phylogenetic signal (Li *et al.* 2020) and several recent matrices have already implemented this notion in their character list (Dieudonné *et al.* 2020; Brown *et al.* 2021; Poole 2022). We adopted a 'guided super matrix approach', in which we condensed several characters from different published datasets: Prieto-Márquez *et al.* (2019), Dieudonné *et al.* (2020), Takasaki *et al.* (2020), and Poole (2022). We further extensively sampled the under-represented areas of the skeleton in the original matrix, focusing on the following anatomical parts: scapular girdle, manual elements, pelvic girdle and axial skeleton (Fig. 1A). In the above-mentioned datasets, these anatomical parts played a major role in the structure of the topology. Lastly, we added or reformulated some characters, including:

Character 91. Carpus, composition of the carpus (after Norman 2015, char. 79) (Fig. 2): (0) composed of some fully ossified and separate carpals, including the ulnare, radiale, intermedium and distal carpals; (1) composed of multiple carpals interlocked together to form a solid carpal block; (2) composed of multiple carpals fused together to form a solid carpal block; (3) reduced to two small separate carpals.

Comments: the carpus is one of the anatomical structures that underwent major transformations during the evolutionary history of iguanodontian dinosaurs, in order to sustain a quadrupedal stance (Maidment & Barrett 2014; Poole 2022). Overall, neornithischians and early-diverging iguanodontians have a carpus composed by several small unfused carpal bones. In some later diverging iguanodontians these elements become progressively larger and show different degrees of fusion between them; in hadrosauroids they become two reduced, unfused elements (Poole 2022).

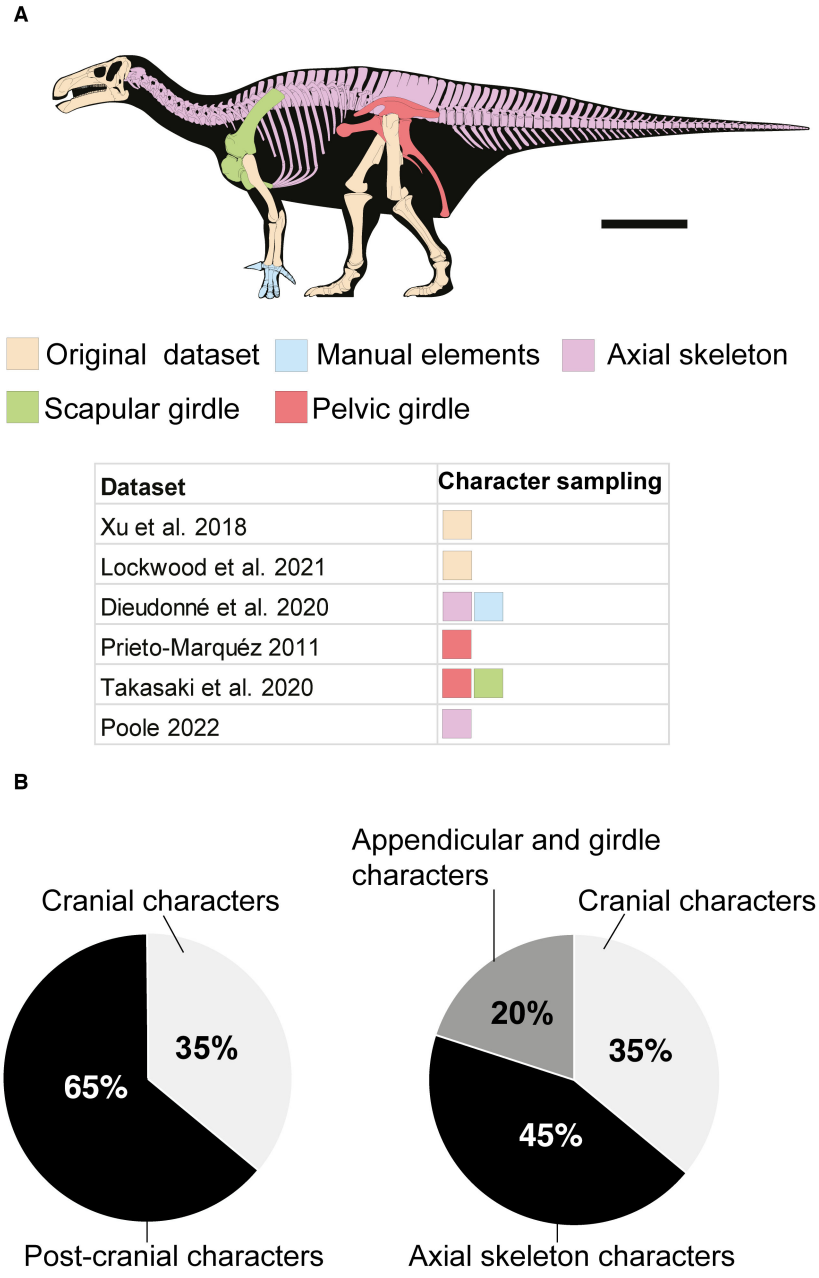

FIG. 1. Illustration of the composition of the dataset. A, the sampled anatomical regions and the original datasets; scale bar represents 1 m. B, the percentage of cranial and postcranial characters. Silhouette: Slate Weasel (CC BY-SA 4.0; Wikimedia Commons).

Several authors have included characters related to this structure in their phylogenetic analyses or anatomical description (Norman 1986; Sereno 1986; Weishampel *et al.* 2003; Poole 2022). However, we modified this character adding a state (1): carpus composed of multiple carpals interlocked together to form a solid carpal block. This condition was addressed for the first time by Rotatori *et al.* (2022) while describing the new carpal material of the holotype of *Draconyx loureiroi*, although they did not provide a formal definition/description of the character. Functionally, the state 0 indicates a grasping hand while states 1 to 3 indicate progressively more rigid structures. We discuss its evolutionary significance later in the corresponding section.

Character 135. Radiale, fusion to the intermedium: (0) absent; (1) partially fused (suture still visible); (2) total fusion (suture obliterated).

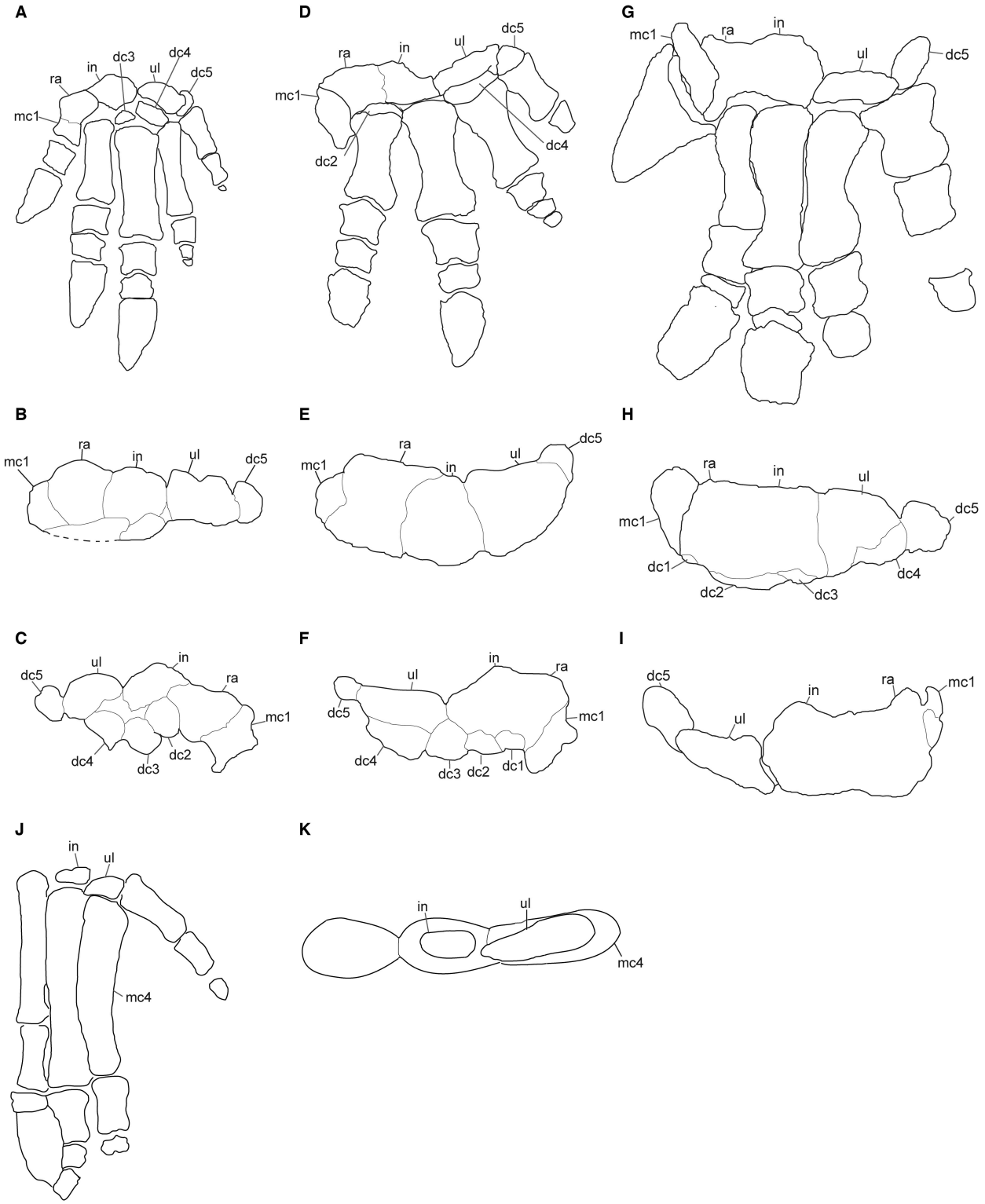

FIG. 2. Illustration of Character 91, composition of the carpus: composed of fully ossified and separate carpals, including the ulnare, radiale, intermedium and distal carpals (A–C), composed of multiple carpals interlocked together to form a single and solid carpal block (D–F), composed of multiple carpals fused together to form a single and solid carpal block (G–I), reduced to two small separate carpals (J–K). Modified from Rotatori et al. (2022); J–K after Tsogtbaatar *et al.* (2019). *Abbreviations*: dc, distal carpal; in, intermedium; mc, metacarpal; ra, radiale; ul, ulnare.

Comments: when commenting on the composition of the carpus, other authors focused on the general degree of fusion of the whole structure, proposing cumulative character states (e.g. Poole 2022). Here we decided to break down the general morphology of the carpus (Char. 91, see above) and this character describes its anatomy more in detail, since different fusion pattern may occur that produce the same carpal structure.

Character 185. Sacral vertebrae, number, including dorsosacrals and sacrocaudals: five or fewer (Fig. 3A), six (Fig. 3B), seven (Fig. 3C), eight or more (Fig. 3D).

Comments: scores on the number of sacral vertebrae are, again, very widespread in phylogenetic matrices (Weishampel *et al.* 2003; Butler *et al.* 2008; Poole 2022). We modified the original character statement from Poole (2022), to include distinct scorings for six, seven and eight or more. The higher number of sacral vertebrae is generally associated with longer iliac blades.

Of the currently included 215 characters (139 of which are postcranial ones, accounting for 64.65% of the total), the majority of these characters include features from the axial skeleton (97 characters) representing 45.12% of the character scorings. Characters related to the appendicular skeleton and girdles (42) represent 19.53% of the total. The 76 cranial characters account for 35.35% of the total (Fig. 1B). The character list was constructed to exclude overweighting and repetition of characters. The following characters were treated as ordered as in the original reference datasets: 140, 141, 142, 143, 144, 145, 146, 147, 148, 149, 150, 151, 152, 154, 155, 156, 157, 158, 159, 160, 175, 177, 187, 201, in both maximum parsimony and Bayesian inference analyses.

Datasets, TNT files, nexus files and scripts to replicate the analyses described here are provided in Rotatori et al. (2026).

Phylogenetic analyses

Maximum parsimony. The dataset produced was analysed using the script of Vila *et al.* (2022) in TNT v1.6 (Goloboff & Morales 2023). We used New Technology search strategies to search for most parsimonious trees (MPTs). We ran a driven search with 10 initial addition sequences, finding the minimum length 10 times. We used 100 rounds sectorial searches, 100 cycles of tree-drifting, 100 cycles of ratchet and 10 rounds of tree fusing, with the following parameters: for sectorial searches we set the minimum size of sectors to five and used random sector selections and 100 cycles of constraint-based selections with a minimal fork of five. For tree-drifting, we explored trees with a max difference in absolute fit of five and a maximum difference in relative fit of 0.1. All other settings were left at their default values. The following command will set TNT v1.6 ready for this analysis:

```
drift : fitdiff 5 rfitdiff 0.1; sectsch : rss minsize 5; sectsch :
  css minfork 5 rounds 100; xmult : rss
  css drift 100 ratchet 100 fuse 10 replications 10 hits 10;
```

We used both equal weighting and extended implied weighting for both datasets. Following Ezcurra (2024) and considering a matrix with fewer than 60 terminal taxa, we explored all concavity constants (k) from 3 to 11 to explore the effect of down weighing homoplasy on the dataset. Strict consensus topologies for $k = 3$–$k = 11$ are provided in Appendix S1. The TNT scripts to reproduce the analyses are provided in Rotatori et al. (2026).

To further test the topological stability of our analyses we used an R script to assess the completeness index of the taxa, which is calculated as:

$$\text{number of scored characters for certain taxon} / \text{total number of characters} \times 100$$

Then we removed the taxa with a completeness index less than 30% and repeated the tree search protocol as above.

Bayesian inference. We performed both non-clock and clock analyses employing Bayesian Inference, with the software MrBayes v3.2.7a run on the CIPRES platform (Ronquist *et al.* 2012b). In the non-clock analysis character evolution followed the Mk model (Lewis 2001) and the values were sampled from a gamma distribution. The analysis sampled 30 000 000 generations per run, sampled with Metropolis-coupled Markov chain Monte Carlo (MCMCMC) method for four runs of four chains per run. The initial 'burn-in' was set at 25%. Convergence of independent runs and stationarity were assessed using the program Tracer v1.7.1 (Rambaut *et al.* 2018) considering effective sample size (ESS) for each parameter informative with values ≥200. Moreover, we assessed potential scale reduction factor (PRSF), average standard deviation of split frequencies (ASDSF) and marginal likelihood, as indicators of the good quality of the analysis.

The clock analysis used the same model for character evolution, while as a clock model we employed the morphological clock (hereafter, 'morphoclock' for sake of simplicity) (Lee *et al.* 2014). To implement morphoclock model into MrBayes we chose a uniform tree model, and we used independent gamma rate as relaxed clock model. Used a mix of tip and node dating, deriving an informative prior from the tip ages for the nodes. Therefore, we did not provide an informative prior for the age of the root, which was derived as any other node within the topology. Absolute age calibrations derived from literature

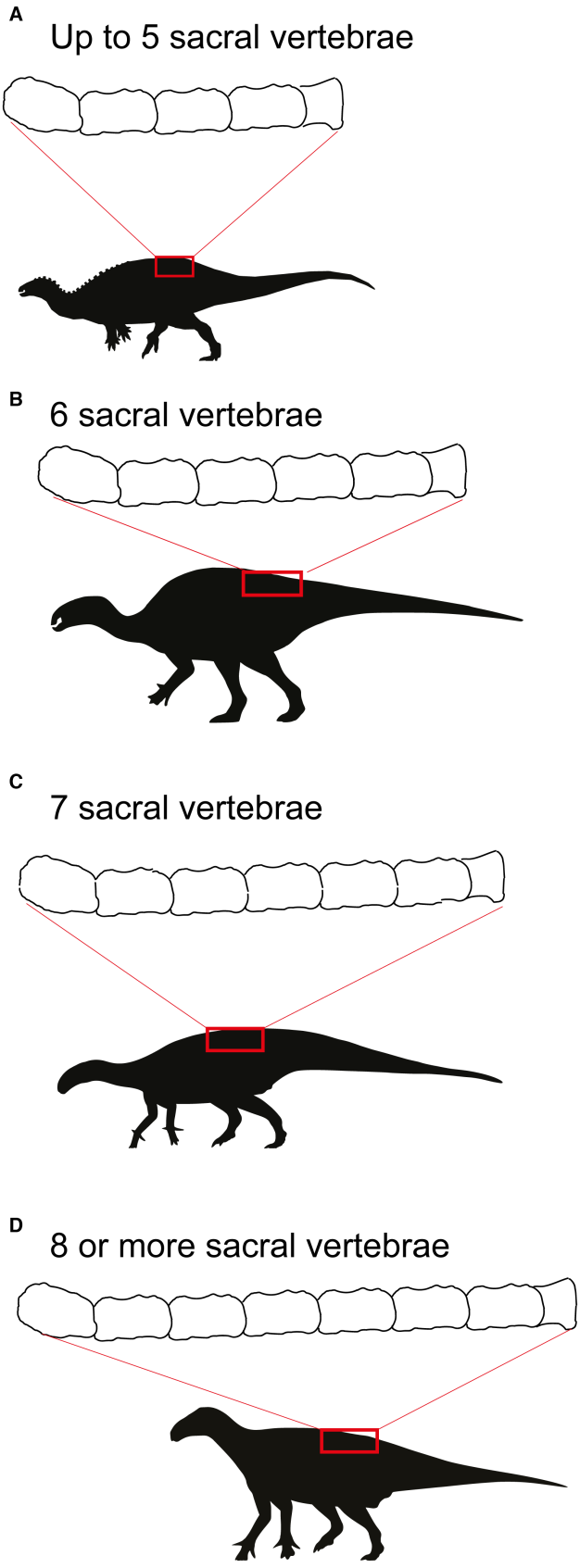

FIG. 3. Illustration of Char. 185, sacral vertebrae, number, including dorsosacrals and sacrocaudals: five or fewer (A), six (B), seven (C), eight or more (D). (Silhouettes from https://www.phylopic.org/: *Camptosaurus dispar*, Tasman Dixon (CC0 1.0); *Equijubus normani*, Pete Buchholz (CC BY-SA 3.0); *Matellisaurus atherfieldensis* (CC BY 3.0), *Iguanadon bernissartensis* (CC BY-SA 4.0), both Matthew Dempsey.)

revision, are provided as raw data (ST2). Stratigraphic ranges were used in combination with FAD/LAD in order to address age uncertainty in the tips (ST2). We chose this character evolution model over other competing ones (e.g. Gavryushkina *et al.* 2014) to avoid over-parametrization of the analysis. The analysis sampled 80 000 000 generations per run, sampled with the MCMCMC method for four runs of four chains per run. The initial 'burn-in' was set at 25%. In order to warrant congruent time-calibration in MrBayes, we created a 'dummy' terminal taxon scored as '?' only for all characters and constrained its position in the topology as a sister taxon of *Hypsilophodon foxii*, then pruned it *a posteriori*. Convergence of independent runs and stationarity were assessed via Tracer v1.7.1 (Rambaut *et al.* 2018). As in the clock analysis, we assessed PRSF, ASDSF and marginal likelihood, as indicators of the good quality of the analysis.

Convergence of independent runs was assessed using: ASDSF (*c.* 0.003 for non-clock analysis, *c.* 0.005 for clock analysis), PSRF = 1 for both analyses, ESS for each parameter was >200 for and marginal likelihood (harmonic mean: −2598.07 for non-clock analysis, −2628.19 for clock analysis). The main divergence times are summarized in Table 2.

To test the robustness of the results, we also ran three more clock analyses in which we adopted different clock priors or using different models. We ran one additional morphoclock model of Lee *et al.* (2014) and two different simple fossilized birth–death (FBD) model analyses (Gavryushkina *et al.* 2014). We left the model choice unaltered for the characters and relative character priors. In the modified version of morphoclock we included a soft upper bound (210, 215) consistent with the stratigraphic range of Ornithischia (Baron 2019; Fonseca *et al.* 2024). The clockrate prior was modelled from the non-clock analysis, subdividing the median value for tree length in substitutions from posterior trees by the age of the tree, based on the average of the distribution for the root prior (7.86/215 = 0.04) following Simões *et al.* (2020a, 2020b). We modelled rates based on a log-normal distribution, with the rates sampled from the log-normal distribution and the mean of the log-normal distribution given the value based on the non-clock tree estimate (0.04) in natural log scale = −3.2188. We chose to use the exponent of the mean to provide a broad standard deviation ($e^{0.04} = 1.040$).

We ran also two FBD model analyses, sampled under diversity strategy, maximizing the probability of modern day taxon sampling ('dummy' taxon) and corrected to avoid sampled-ancestor option. One analysis retained the clock priors used in the first morphoclock analysis, while the second FBD implemented the clock priors of the modified version of the morphoclock analysis. A summary of the Bayesian sensitivity tests are provided in Appendix S1.

The scripts to replicate non-clock and clock analyses are provided in Rotatori et al. (2026).

Character modelling

Historical biogeography. To reconstruct the historical biogeographic history of iguanodontians, we employed the maximum compatibility tree (MCT) from the clock analysis, and used the R package BioGeoBEARS (Matzke 2018) to test which biogeographical model best fits the evolutionary history of Iguanodontia: we tested for DIVALIKE and DIVALIKE + j, DEC and DEC + j, BAYAREALIKE and BAYAREALIKE + j. These models incorporate key phenomena involved in historical biogeography, like dispersal and vicariance (DIVALIKE, modelling dispersal and vicariance events, but does not include sympatric-subset speciation events), founder effect with jump dispersal (the j indicates a founder-event 'jump' speciation modelled as additional parameter), dispersal-extinction and cladogenetic events (DEC) and lastly dispersal, extinction and sympatry (BAYAREALIKE) (Matzke 2014). Each taxon was scored for the following five areas: North America, South America, Europe, Asia and Africa. We used a dispersal matrix with pairwise dispersal multipliers that considers different dispersal probabilities between land masses as tectonic evolution progressed throughout the Mesozoic (i.e. time-stratified analysis), with main continental reconfigurations differently set at intervals between 152, 123, 117, 100, 90, 72 and 66 Ma based on palaeogeographic constraints in Upchurch & Chiarenza (2024). Following these palaeogeographic constraints, connectivity scores were embedded in a dispersal matrix in which values near 1 indicate an almost continuous land connection (e.g. Europe–Asia), whereas values approaching 0 mark strong oceanic barriers or insurmountable dispersal distance for a terrestrial tetrapod (e.g. Asia – South America).

TABLE 2. Divergence times for major clades within Iguanodontia recovered from different analyses.

Model	Clockrate prior	Informative root prior	Root	Iguanodontia	Dryomorpha	Ankylopollexia	Styracosterna	Hadrosauroidea
Morphoclock	**Normal distribution**	**No**	**191**	**186.5**	**183.7**	**178.1**	**174.9**	**149.6**
Morphoclock	Derived from NC	Yes	213	207	203	199.6	195.9	162
FBD	Normal distribution	No	192	167.8	164.2	155.7	152	128
FBD	Derived from NC	Yes	211	171.6	166.8	156.1	153.5	129.4

FBD, fossilized birth–death; NC, non-clock analysis. Bold text indicates model discussed in detail.

BioGeoBEARS was instructed to let each lineage occupy at most two areas simultaneously; composite states such as Europe + Africa were therefore allowed when the ancestral-state reconstruction implied a broadly distributed ancestor. We employed Akaike information criterion with finite correction (AICc) (Sugiura 1978) and AIC weights (Burnham & Anderson 2002) to choose the best fitting model (i.e. the model exhibiting the lowest AICc, thus the highest AICc weight was considered the best-supported fit to the data), see Table 3.

We provide dispersion matrix probabilities alongside with the script and the data to replicate the analyses, as well as the raw results of all five models in Rotatori et al. (2026).

Institutional abbreviations. AMNH, American Museum of Natural History, New York, NY, USA; CM, Carnegie Museum of Natural History, Pittsburgh, PA, USA; GPIT, Geologisch-Paläontologisches Institut der Eberhard-Karls-Universität Tübingen, Germany; IWCMS, Isle of Wight County Museum Service (MIWG, Museum of Isle of Wight Geology, was used for accessions prior to 1994), Dinosaur Isle Museum, Isle of Wight, UK; MAP, Museo Aragonés de Paleontología, Teruel, Spain; ML, Museu da Lourinhã, Lourinhã, Portugal; MNS, Museo Numantino de Soria, Spain; NHMUK, Natural History Museum, London, UK; MPT, Museo de Teruel, Spain; OUMNH, Oxford University Museum of Natural History, UK; RBINS, Royal Belgian Institute of Natural Sciences, Brussels, Belgium; SHN, Sociedade de História Natural, Torres Vedras, Portugal; SMNS, Staatliches Museum für Naturkunde, Stuttgart, Germany; USNM, National Museum of Natural History, Smithsonian Institution, Washington DC, USA; YPM, Yale Peabody Museum, New Haven, CT, USA.

RESULTS: PHYLOGENETIC ANALYSIS

Maximum parsimony

The equal weighting analysis returned 32 trees of 643 steps (consistency index = 0.473, retention index = 0.788, rescaled consistency index = 0.373). Hereafter we describe some of the most important topological features illustrated in the strict consensus tree (Fig. 4). The earliest diverging clade within Iguanodontia is Rhabdodontidae, which includes *Iani smithi*, *Rhabdodon* sp., *Zalmoxes shqiperorum* and *Zalmoxes robustus* as in many recent phylogenetic analyses (e.g. Zanno *et al.* 2023). Synapomorphies of this clade are the well-developed primary ridge on the labial surface of dentary teeth, becoming less prominent apically (Char. 70: 0>1); wide maxillary crowns, albeit still smaller than dentary crowns (Char. 73: 0>1); ventral sulcus absent on caudal centra (Char. 191: 0>1).

In this topology, *Tenontosaurus tilletti* is sister taxon to Dryomorpha, as commonly found by other workers (Xu *et al.* 2018; Maidment *et al.* 2022; Poole 2022; Rotatori *et al.* 2022; Bonsor *et al.* 2023). Within Dryosauridae, we recovered *Valdosaurus canaliculatus*, *Dysalotosaurus lettowvorbecki*, *Dryosaurus altus* and *Eousdryosaurus nanohallucis*, the latter two taxa are recovered as sister taxa (synapomorphies: ventral margin of the coracoid relatively blunt and roughly right-angled, Char. 86: 0>1). *Cumnoria prestwichii* is recovered sister to Ankylopollexia, as in (Maidment *et al.* 2022). The earliest diverging members of Ankylopollexia are *Oblitosaurus bunnueli*, *Camptosaurus dispar* and the SHN specimen. The placement of *O. bunnueli* contrasts with the its original description of Sánchez-Fenollosa *et al.* (2023) in being more deeply nested within Ankylopolexia, and actually being recovered as a member of Styracosterna. Notably, this species was not recovered as sister to *Draconyx loureiroi*. We recovered a 'high-sailed' styracosternans clade sister to Hadrosauriformes, which includes *Brighstoneus simmondsi*, *Ouranosaurus nigeriensis* and *Morelladon beltrani* (synapomorphies: neural spine centred in dorsal centra, Char. 129: 1>0; very tall neural spine relative to centrum, and compared to tallest caudal, dorsal or sacral Char. 140: 0>2; caudodorsally oriented dorsal margin of post-acetabular process, rising dorsally relative to the acetabular margin, Char. 150: 0>1).

TABLE 3. Model log-likelihood (lnl) scores with Akaike information criterion (AIC) scores for BioGeoBEARS models.

Model	LnL	*k*	AIC	AICc	deltaAICc	AICc_wt
DEC	−95.6008	2	195.2016	195.4516	15.0094542	0.0004713
DEC + j	**−86.9658**	**3**	**179.9316**	**180.4422**	**0**	**0.8562486**
DIVALIKE	−95.9961	2	195.9922	196.2422	15.799986	0.0003175
DIVALIKE + j	**−88.7571**	**3**	**183.5141**	**184.0247**	**3.58254434**	**0.1427777**
BAYAREALIKE	−112.786	2	229.5715	229.8215	49.3793199	1.62E-11
BAYAREALIKE + j	−95.4062	3	196.8124	197.323	16.8807957	0.0001849

The two best supported models are shown in bold (the best model is DEC + j).

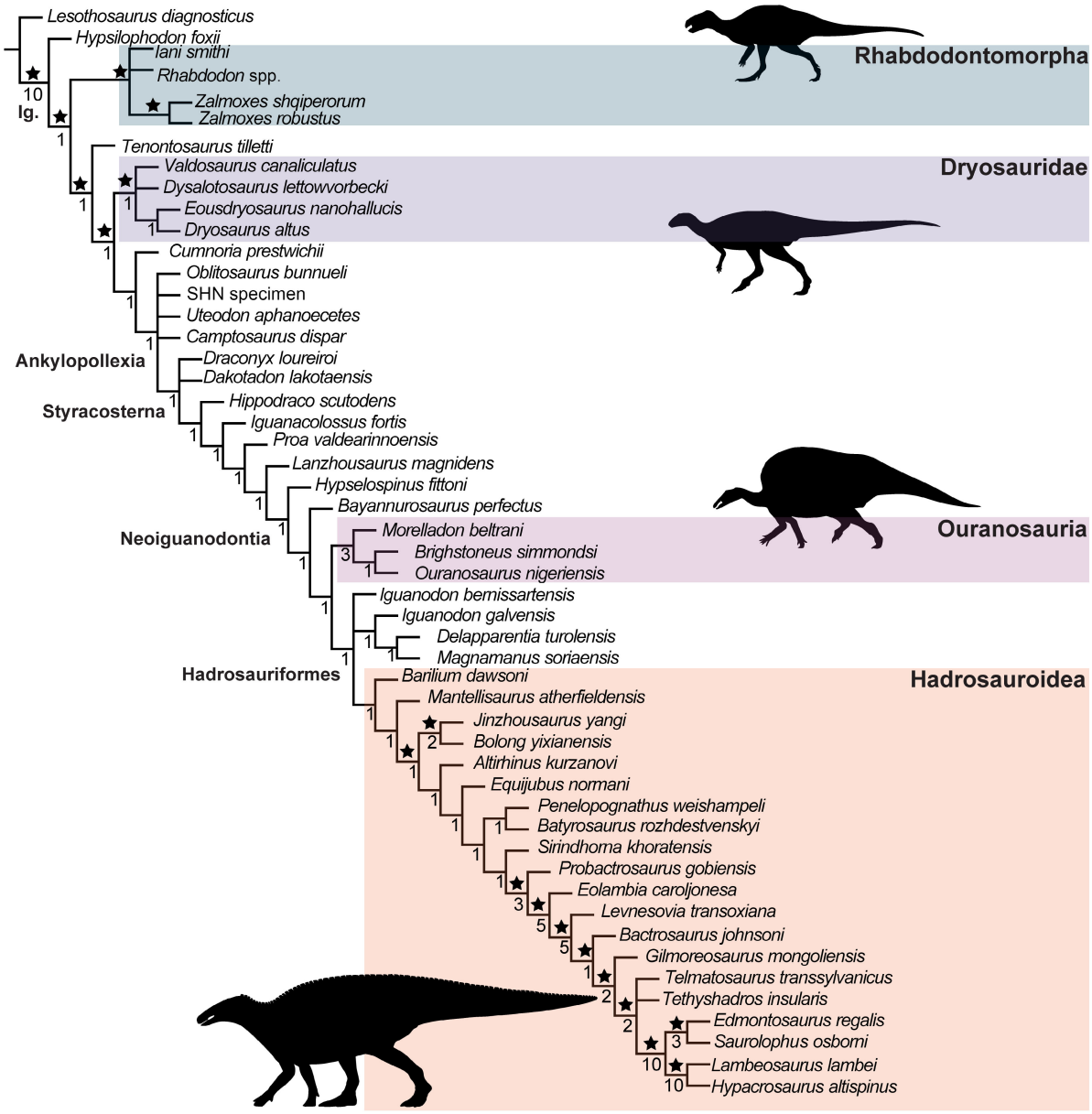

FIG. 4. Strict consensus tree of the maximum parsimony analysis employing equal weighting. Numbers are Bremer support values, star symbols indicate Bootstrap values >50%. *Abbreviation*: Ig., Iguanodontia. (Silhouettes from https://www.phylopic.org/: *Zalmoxes robustus* (CC BY 3.0); Scott Hartman; *Dysalotosaurus lettowvorbecki*, Matthew Dempsey (CC BY 4.0); *Ouranosaurus nigeriensis*, Scott Hartman (CC BY-NC-SA 3.0) *Edmontosaurus annectens*, Matthew Dempsey (CC BY 3.0).)

We did not recover a monophyletic *Iguanodon* clade as Verdú *et al.* (2017a); instead, we recovered all the Iberian styracosternans nested within the same clade, which comprises of '*Iguanodon*' *galvensis*, *Magnamanus soriaensis* and *Delapparentia turolensis* (synapomorphies: coronoid process of dentary perpendicular to the dorsal edge of the dentary ramus Char. 52: 0>1; shape of the apex of the coronoid process of dentary in lateral or medial view suboval and anteroposteriorly expanded Char. 53: 1>0). *Mantellisaurus atherfieldensis* and *Barilium dawsoni* are recovered as more deeply nested than other hadrosauriforms being the earliest diverging branches of Hadrosauroidea. Synapomorphies of Hadrosauroidea are: the curvature of the femoral shaft moderately bent posteromedially along the proximal half of the shaft (Char. 115: 1>0); a lateral profile of the dorsal or laterodorsal margin of the ilium distinctly depressed over the supraacetabular process and dorsally bowed over the proximal region of the preacetabular process (Char. 152: 0>1).

The other extended implied weighting analyses (Fig. 5) recovered a similar topology of the consensus tree, despite the relatively high homoplasy identified in the dataset, with CI below 0.5 for all most parsimonious trees. All trees recovered a well-resolved Ankylopollexia and successive nested clades, with differences observed towards the root of the tree, characterized by the higher density in homoplasy. The strongest down weighing of the homoplasy ($k = 3$) recovered *Brighstoneus simmondsi* as the earliest diverging member within Hadrosauroidea, a poorly resolved Dryosauridae and the putative rhabdodontomorph *Iani smithi* within Ankylopollexia. Concavity constants larger than 4 recovered almost the same topology, but interestingly for this work, the high sailed *Brighstoneus simmondsi* is recovered in a clade with *Ouranosaurus nigeriensis* and *Morelladon beltrani*. Once the k value goes over 7, Dryosauridae is partially resolved, with *Dryosaurus altus* and *Eousdryosaurus nanohallucis* forming a clade. Finally, large concavity constants (from $k = 9$ to $k = 11$) stabilize and show the last change in the topology, with *Iani smithi* recovered at the base of Rhabdodontomorpha, the clade in which was originally described.

The extended implied weighting analysis with $k = 11$ returned one single tree of 644 steps (consistency index = 0.472, retention index = 0.787, rescaled consistency index = 0.371). The topology is mostly consistent with the equal weighting analysis (see Figs S4–S10), although we note some important differences. *Oblitosaurus bunnueli* is here recovered as styracosternan, more deeply nested than *Camptosaurus dispar* and the SHN specimen (synapomorphy: morphology of the fourth trochanter of femur slightly mediolaterally thick and subtriangular, Char. 116: 0>1), differing from the original placement of Sánchez-Fenollosa *et al.* (2023). *Mantellisaurus atherfieldensis* and *Barilium dawsoni* are recovered as earliest diverging members of the clade Iguanodontidae, which includes the Iberian styracosternans '*Iguanodon*' *galvensis*, *Delapparentia turolensis* and *Magnamanus soriaensis* (synapomorphy: preacetabular process moderately axially twisting so that the lateral surface of the process faces dorsolaterally, Char. 100: 0>1).

The rest of the topology does not differ significantly from that of the original matrix and subsequent iterations (Xu *et al.* 2018; Lockwood *et al.* 2021, 2024; Maidment *et al.* 2022; Rotatori *et al.* 2022, 2025; Bonsor *et al.* 2023; Sánchez-Fenollosa *et al.* 2023).

The sensitivity test after the removal of the taxa <30% complete did not produce any evident difference with the main maximum parsimony analysis (Fig. S1).

Bayesian inference

The non-clock analysis returned a topology largely consistent with the maximum parsimony analyses (see the maximum compatibility tree, Fig. S14).

One of the main differences between the non-clock analysis and the others is the placement of *Iani smithi*, which is not recovered within Rhabdodontidae (Zanno *et al.* 2023), but as sister to the node *Tenontosaurus tilletti* + Dryomorpha. *Draconyx loureiroi* and *Cumnoria prestwichii* are recovered as sister taxa, diverging earlier of the node Ankylopollexia. Both the SHN specimen and *Oblitosaurus bunnueli* in this analysis are recovered within Styracosterna, more deeply nested than of both original descriptions (Sánchez-Fenollosa *et al.* 2023; Rotatori *et al.* 2025). As in the maximum parsimony analysis, the clade of high-sailed styracosternans (*Ouranosaurus nigeriensis*, *Morelladon beltrani* and *Brighstoneus simmondsi*) is recovered (synapomorphies: morphology of the dorsal edge at the joint between the central plate and postacetabular process of ilium, dorsoventrally thickened and laterally bulgy, forming a non-everted, weakly developed eminence, Char. 102: 2>3; central length of cervical vertebrae remains approximately the same or decrease posteriorly, Char. 129: 1>0; very tall neural spine relative to the centrum, relative to tallest caudal, dorsal or sacral, Char. 140: 0>2; caudodorsally oriented dorsal margin of post-acetabular process, rising dorsally relative to the acetabular margin, Char. 150: 0>1; absence of a ventral sulcus on the ventral surface of caudal centra, Char. 191: 1>0; subequal facets of chevrons, Char. 198: 0>1). *Barilium dawsoni* is recovered within Iguanodontidae, a clade recovered in this analyses with *Iguanodon bernissartensis* + ('*Iguanodon*' *galvensis* + (*Delapparentia turolensis* + *Magnamanus soriaensis*)) as members (synapomorphies: coronoid process of dentary perpendicular to the dorsal edge of the dentary ramus,

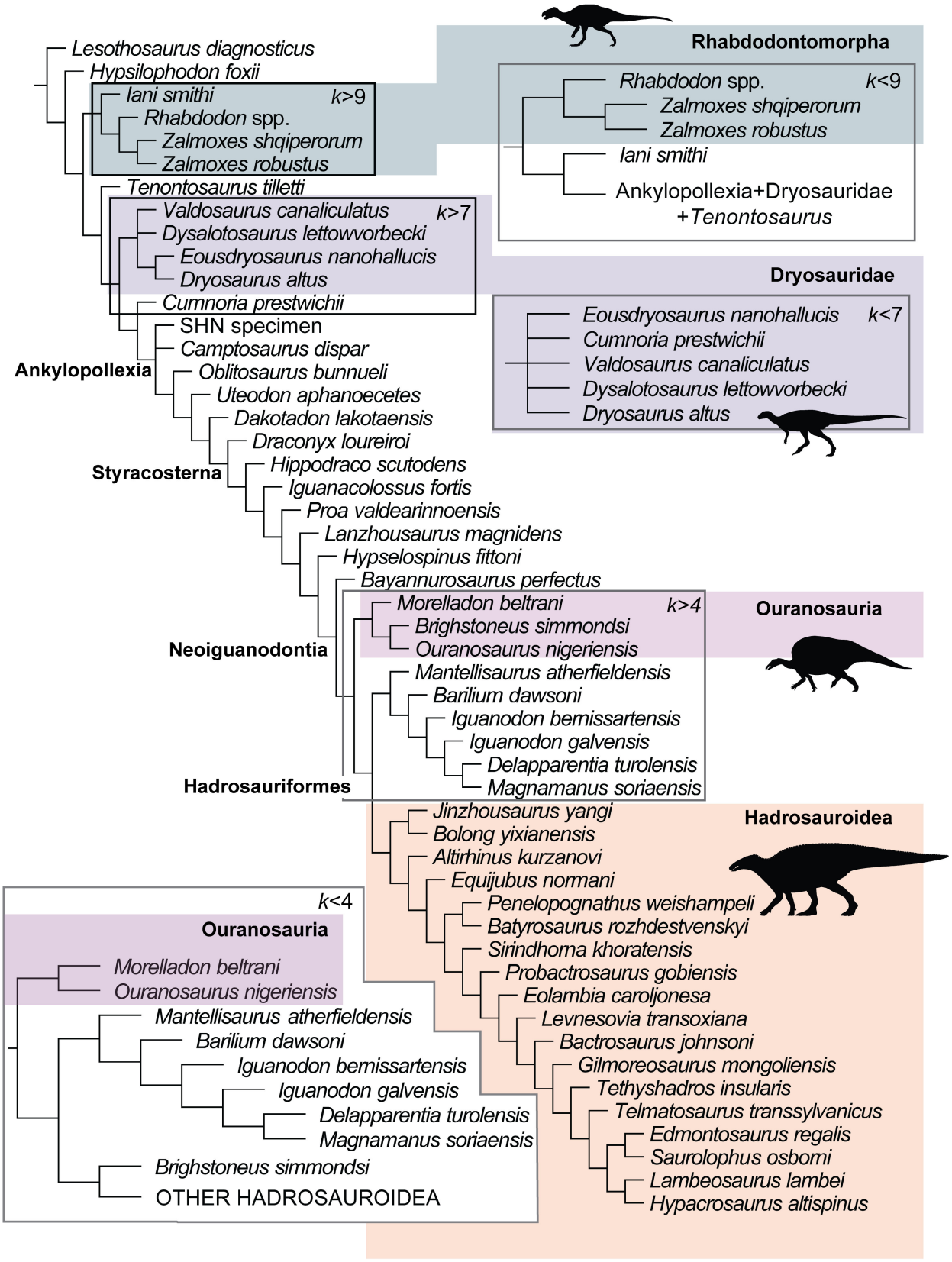

FIG. 5. Strict consensus tree of the maximum parsimony analysis employing extended implied weighting with concavity constant $k = 11$, and missing entries having half of the homoplasy of observed entries, capped at 4. Parts of the tree that show changes in topology with lower concavity constants are highlighted in black bordered boxes and the corresponding alternative topology is shown in grey bordered boxes, indicating the value of k at which the topological change occurs. For topologies of each consensus tree from $k = 3$ to $k = 11$, see Appendix S1. (Silhouettes from https://www.phylopic.org/: *Zalmoxes robustus* (CC BY 3.0); Scott Hartman; *Dysalotosaurus lettowvorbecki*, Matthew Dempsey (CC BY 4.0); *Ouranosaurus nigeriensis*, Scott Hartman (CC BY-NC-SA 3.0) *Edmontosaurus annectens*, Matthew Dempsey (CC BY 3.0).)

Char. 52: 0>1; shape of the apex of the coronoid process of dentary in lateral or medial view sub-oval and antero-posteriorly expanded, Char. 53: 1>0). *Mantellisaurus atherfieldensis* is recovered as the earliest diverging member of Hadrosauroidea, as in Bonsor *et al.* (2023). The rest of the topology does not differ significantly from previous iterations of the original matrix (Xu *et al.* 2018; Lockwood *et al.* 2021, 2024; Maidment *et al.* 2022; Rotatori *et al.* 2022, 2025; Bonsor *et al.* 2023; Sánchez-Fenollosa *et al.* 2023).

The clock analysis (Fig. 6) presents some topological differences compared to other analyses as well. Considering the topology of the MCT (Fig. 6), *Tenontosaurus tilletti* is recovered within Rhabdontomorpha, alongside *Iani smithi* and Rhabdodontidae, consistent with previous studies (Poole 2022; Zanno *et al.* 2023). *Camptosaurus dispar* and *Uteodon aphanoecetes* are recovered as sister taxa, as *Hypselospinus fittoni* is recovered sister to the node *Lanzhousaurus magnidens* + *Bayannurosaurus perfectus*. The clade of high-sailed styracosternans remains unaltered (synapomorphies: curvature of the femoral shaft in antero-posterior view absent – nearly straight diaphysis – along the entire shaft, with a slightly medially curved proximal third, Char. 115: 0>1; central length of cervical vertebrae remains approximately the same or decrease posteriorly throughout the series, Char. 129: 1>0; very tall neural spine relative to centrum, and in comparison to tallest caudal, dorsal or sacral, Char. 140: 2; caudodorsally oriented dorsal margin of post-acetabular process, rising dorsally relative to the acetabular margin, Char. 150: 1; absence of a ventral sulcus on the ventral surface of caudal centra Char. 191: 0), whereas we recover *Mantellisaurus atherfieldensis* + *Barilium dawsoni* sister to Iguanodontidae, which includes Iberian styracosternans (synapomorphies: coronoid process of dentary perpendicular to the dorsal edge of the dentary ramus, Char. 52: 0>1; shape of the apex of the coronoid process of dentary in lateral or medial view suboval and antero-posteriorly expanded, Char. 53: 1>0). These results are found consistently also in the sensitivity tests employing different Bayesian models (Figs S1–S4).

We note that most of the clades have long ghost-lineages, of at least 10 million years; the earliest divergence times allocated between the Early and the Middle Jurassic. This may be due to the clock model selection, which may be biased to allocate older divergence times at earlier diverging nodes (e.g. Crisp *et al.* 2014; dos Reis *et al.* 2016). The sensitivity tests employing different clock and tree models returned minor incongruences in the topology; the difference is very marked regarding divergence-times for major clades, confirming that model selection has had a significant impact on divergence-times estimation (see Table 2). In general, FBD models return younger divergence times compared to morphoclock ones, recovering divergence times that are more closely aligned with the known sampled age ranges of fossil taxa, hence presenting a more 'literal reading' of the fossil record in their (FBD) outputs (Ronquist *et al.* 2012a; Ho *et al.* 2015; Zhang 2022).

We remark that the results of the present original analysis are in agreement with the work of Rotatori *et al.* (2023), in which the application of a Skyline FBD model on a different dataset (a modified version of the matrix of Dieudonné *et al.* 2020) found congruent results. Furthermore, clock-rates are overall constant through all the topology, with the exception of the initial radiation of Iguanodontia (186 Ma, in the Pliensbachian) and the appearance of later-diverging hadrosauroids (Hadrosauridae). This may be an artefact due to the taxon-sampling of this specific dataset, although we note that other specialists recovered an acceleration in evolutionary rates coinciding to the appearance of hadrosaurids (Stubbs *et al.* 2019; Chiarenza *et al.* 2021, 2024).

The rest of the topology does not differ significantly from previous iterations of the original matrix and subsequent iterations (Xu *et al.* 2018; Lockwood *et al.* 2021, 2024; Maidment *et al.* 2022; Rotatori *et al.* 2022, 2025; Bonsor *et al.* 2023; Sánchez-Fenollosa *et al.* 2023).

SYSTEMATIC PALAEONTOLOGY

As mentioned in previous paragraphs, in all the analyses we recovered a clade that we previously referred to as 'high-sailed styracosternans'. Due to the consistency in the results obtained and high support values for this clade, we propose hereafter the formal erection of the clade according to the PhyloCode standards.

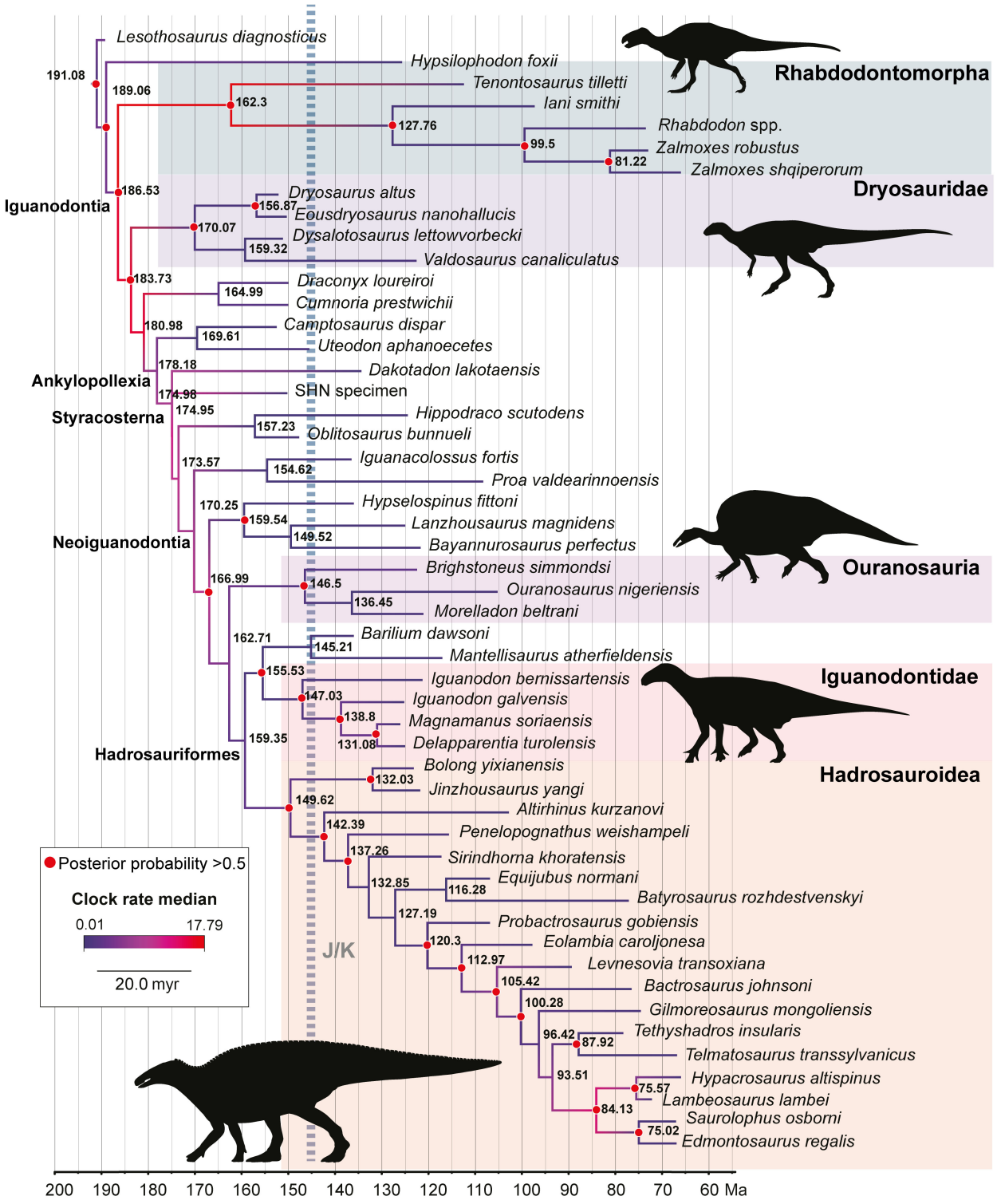

FIG. 6. Maximum compatibility tree (MCT) from the time-calibrated Bayesian inference analysis. Numbers represent diverging times for each node. Red dots indicate posterior probabilities values >0.5. Evolutionary rates are mapped on the tree as clock-rate median. (Silhouettes from https://www.phylopic.org/: *Zalmoxes robustus* (CC BY 3.0); Scott Hartman; *Dysalotosaurus lettowvorbecki*, Matthew Dempsey (CC BY 4.0); *Ouranosaurus nigeriensis*, Scott Hartman (CC BY-NC-SA 3.0); *Iguanadon bernissartensis* (CC BY-SA 4.0) Matthew Dempsey; *Edmontosaurus annectens*, Matthew Dempsey (CC BY 3.0).)

DINOSAURIA Owen 1842
ORNITHISCHIA Seeley 1888b
ORNITHOPODA Marsh 1881
IGUANODONTIA (Sereno 1986)
STYRACOSTERNA Sereno 1986
OURANOSAURIA nov.

Definition. The largest clade containing *Ouranosaurus nigeriensis* Taquet 1976 but not *Iguanodon bernissartensis* Boulenger 1881 or *Hadrosaurus foulkii* Leidy 1858.

Reference phylogeny. Figure 4 (this work), maximum parsimony analysis.

Composition. In all the analyses, the taxa *Ouranosaurus nigeriensis* and *Morelladon beltrani* are recovered within the clade. *Brighstoneus simmondsi* is also present in this clade in all analyses, with the exception of those with very low concavity constants used for downweighing homoplasy ($k \leq 3$).

Synonyms. No other taxon names are currently in use for the same or approximate clade.

Remarks. The affinity of *Brighstoneus simmondsi* and *Ouranosaurus nigeriensis* were first recovered by Lockwood *et al.* (2021) in their 50% majority rule consensus tree (Lockwood *et al.* 2021, fig. 23c), although this analysis did not include *Morelladon beltrani*, which previous analysis recovered as an indeterminate ankylopollexian (Gasulla *et al.* 2015). Bertozzo *et al.* 2025 also recovered *Morelladon beltrani* in a clade with *Oranousaurus nigeriensis*. In this case though, *Brighstoneus simmondsi* was recovered in a more nested position.

The Bremer support values for maximum parsimony are 3 for equal weighting analysis, but 1 for implied weighting $k = 11$. Analyses employing Bayesian inference recovered posterior probabilities >0.50 for this clade.

All the parsimony analyses recovered the following synapomorphies: neural spine of the dorsal vertebrae centred over centrum, high dorsal neural spine (Fig. 7) and caudodorsally oriented post-acetabular process. The Bayesian analyses recovered the presence of a nearly straight curvature of the femoral shaft in anteroposterior view, with a slightly medially curved proximal third, dorsal edge of the ilium at the joint between the central plate and postacetabular process is dorsoventrally thickened and laterally bulgy, forming a well-developed eminence that has a slightly everted, more laterally expanded posterior half, caudal vertebrae without sulcus on ventral surface, craniocaudal length of the distal facets for chevrons on proximal caudal vertebrae are longer than the ventral surface of the vertebrae.

Historical biogeographic reconstruction. We ran the historical biogeographic analysis only employing the original morphoclock analysis, excluding the sensitivity analyses since they produced too unrealistic divergence times (Fig. S2) or presented polytomies that had to be artificially resolved (Figs S3, S4). The two best-supported models are DEC + j (AICc = 180.44) and DIVALIKE + j (AICc = 184.03) (Table 3). Because the DIVALIKE + j (dispersal-vicariance, no sympatry + jump founder effect) model (Ronquist 1997) often outperforms alternative model classes in AIC-based comparisons (Matzke 2014), we report results from both DEC + j and DIVALIKE + j, to ensure that our conclusions are not contingent on a single modelling framework (Fig. 8). The DEC + j model combines the classic Dispersal-Extinction-Cladogenesis events with the founder-effect speciation mechanism (Matzke 2014). The origin of Iguanodontia is recovered in Europe in the Early Jurassic, around 186 million years ago (Pliensbachian). The first occurrence in the fossil record of a definitive iguanodontian is dated to the Callovian of Europe (Ruiz-Omeñaca *et al.* 2006), implying a ghost lineage of approximately 20–30 million years. This starkly contrasts with previous analyses, regarding both the diverging times and geographical context (Boyd 2015; Poole 2022). Our analysis recovered several cladogenetic events that indicate Europe as the main diversification area for the clade with dispersals from there towards North America (since the Middle Jurassic) and later (from the Late Jurassic) towards Asia. The earliest branch dispersing in North America is Rhabdontomorpha, more precisely the lineage that gave rise to *Tenontosaurus tilletti* being the first fossil evidence of such dispersal. Later, iguanodontians continued to diversify in Europe, and both Dryosauridae and Ankylopollexia appeared in North America around 180 million years ago, in the Toarcian. This appears in stark contrast with a literal reading of the fossil record, since the very first ankylopollexians recognizable as such appear not earlier than the Late Jurassic (Norman 2004). Both of these clades dispersed in the Jurassic in other parts of Laurasia (North America) and Gondwana (Africa). Styracosternans originated in North America in the Middle Jurassic around 174 million years ago, in the Aalenian stage, but subsequently dispersed and radiated in Europe, dispersing for the first time in Asia during the Oxfordian–Kimmeridgian. Similarly to Ankylopollexia, the first definitive fossils recognizable as styracosternans are dated either to the Late Jurassic or to the Early Cretaceous, depending on different systematic views (McDonald 2012; Carpenter & Galton 2018), implying an extensive ghost lineage for this group. Ouranosauria and Iguanodontidae evolved and co-existed in Europe; their origin is estimated to be in the Tithonian stage (Fig. 4), but the first dispersal into Gondwana is represented by the *Ouranosaurus nigeriensis* lineage. Of both clades, we

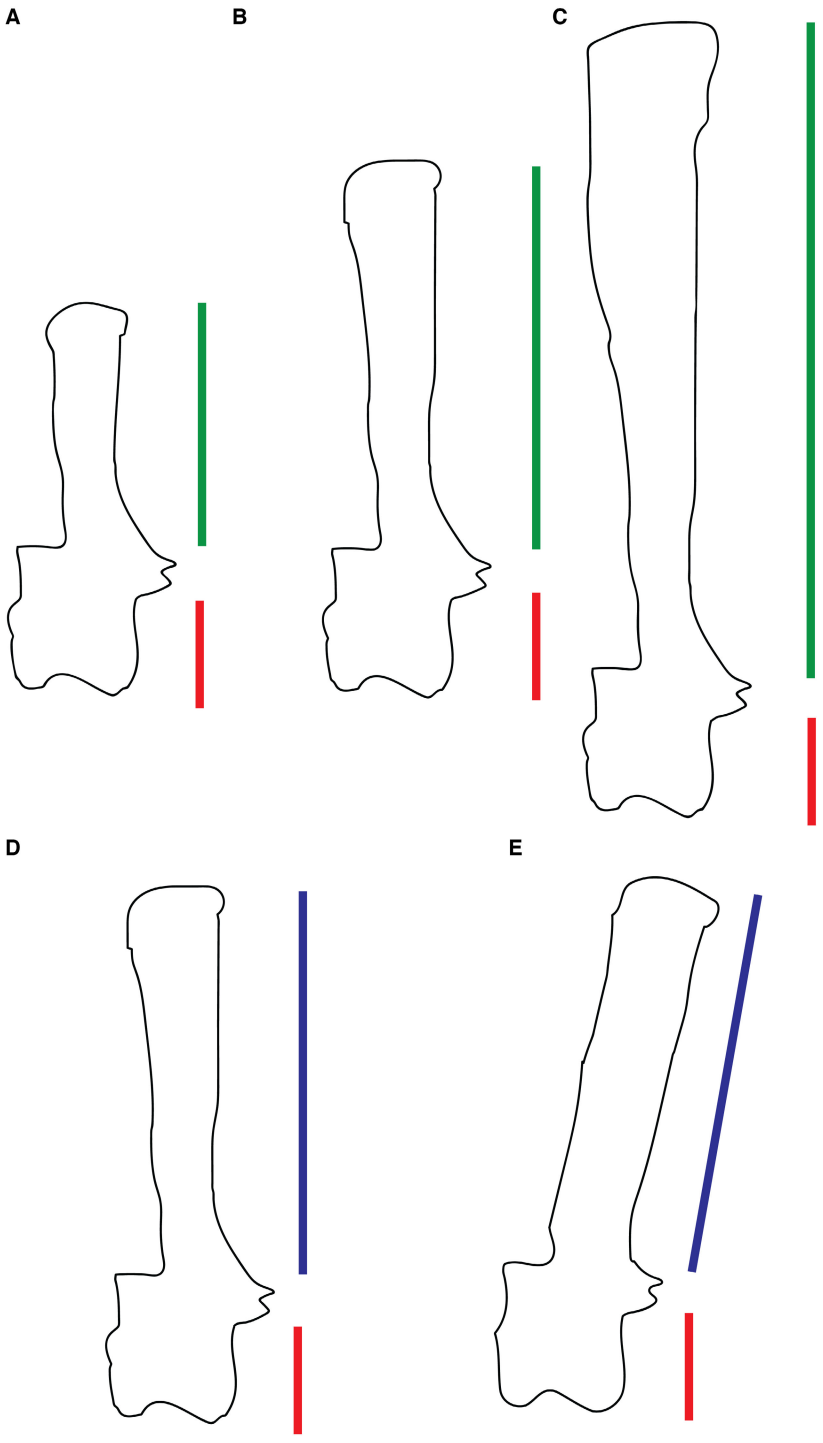

FIG. 7. Illustration of characters 140 (A–C) and 129 (D–E), some of the main synapomorphies of Ouranosauria. Character 140, height of the neural spine relative to that of the centrum of the tallest caudal dorsal or sacral vertebrae: short neural spine, ratio up to 2.10 (A), ratio 2.10 and up to 3.25 (B) and very long neural spine, ratio greater than 3.25 (C). Character 129, dorsal vertebrae, neural spine: anteriorly positioned or centred over the dorsal centrum (D), starting to project posteriorly to their own centrum at some point within the dorsal vertebral series (E).

still do not have sampled fossils dated to the Jurassic, but their Early Cretaceous presence implies a compatible ghost lineage tracing back to at least the latest Jurassic (Norman 2004, 2012; Ruiz-Omeñaca 2011; Gasulla *et al.* 2015; Verdú *et al.* 2015; Vidarte *et al.* 2016; Lockwood *et al.* 2021).

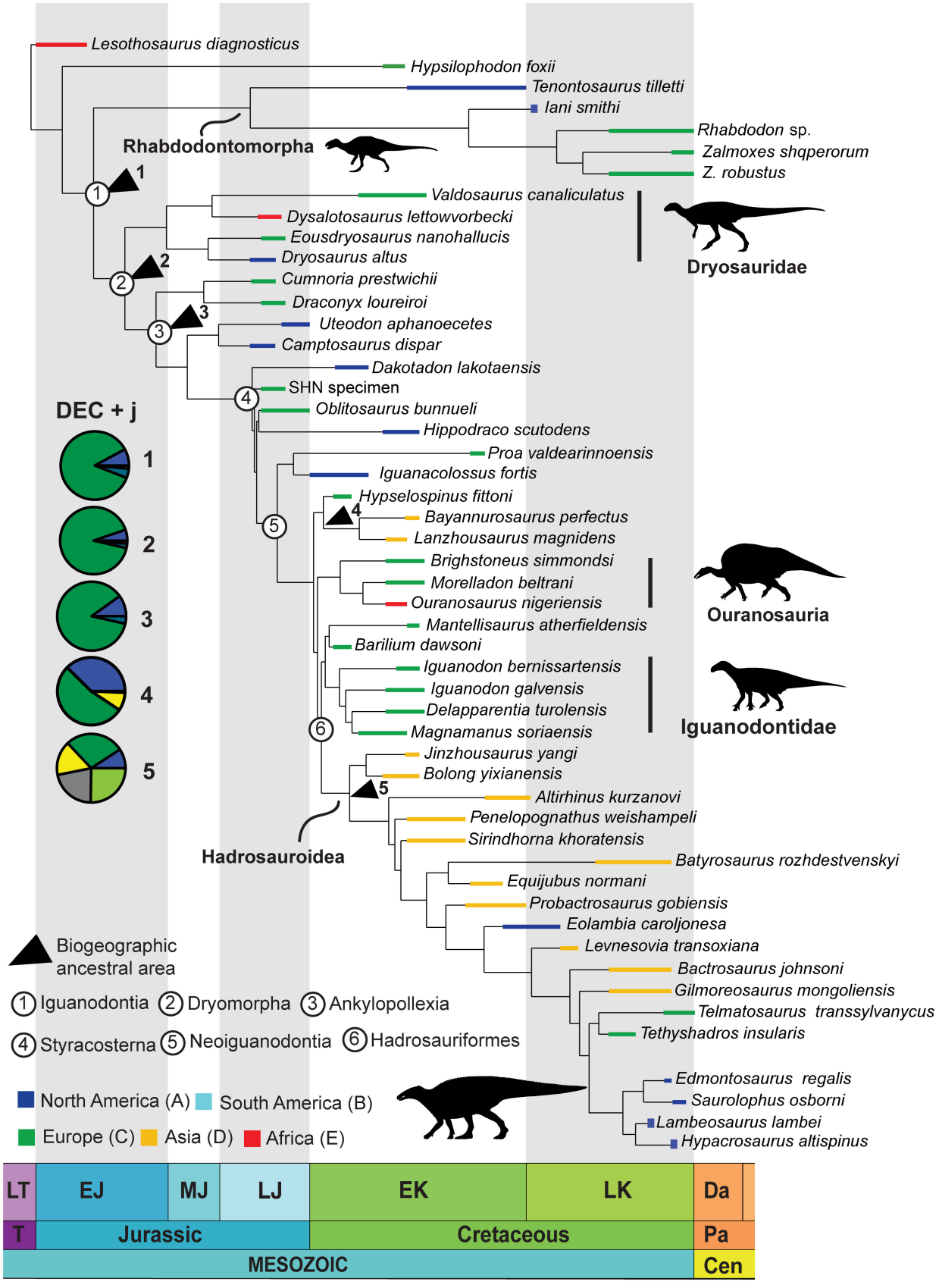

FIG. 8. Historical biogeographic reconstruction of Iguanodontia, employing the DIVALIKE + j model chosen by the BioGeoBears analysis using the time calibrated MCT. Major biogeographic events are indicated across the topology by numbered arrows, with ancestral areas represented by the pie charts; circled numbers represent main clades in Iguanodontia. (Silhouettes from https://www.phylopic.org/: *Zalmoxes robustus* (CC BY 3.0); Scott Hartman; *Dysalotosaurus lettowvorbecki*, Matthew Dempsey (CC BY 4.0); *Ouranosaurus nigeriensis*, Scott Hartman (CC BY-NC-SA 3.0); *Iguanadon bernissartensis* (CC BY-SA 4.0) Matthew Dempsey; *Edmontosaurus annectens*, Matthew Dempsey (CC BY 3.0).)

Hadrosauroidea dispersed out of Europe into Asia (Late Jurassic, *c.* 145 Ma) and North America (before the Early–Late Cretaceous transition, *c.* 115–110 Ma) and, besides the sporadic re-immigration to North America from Europe of the lineage represented by *Eolambia caroljionesa*, it mainly diversified in Asia. Later diverging forms dispersed into North America by the Albian, 112 million years ago. The clade of *Telmatosaurs transsylvanicus* and *Tethyshadros insularis* from the 'Transylvanian islands' and the Adriatic Carbonate Platforms, is the first lineage of hadrosauroids to reappear in Europe from Asia, by the Conacian, around 87 million years ago. Hadrosauridae are here interpreted to have first originated and diversified in North America in the Late Cretaceous, around 84 million years ago, during the Santonian stage.

Character evolution. We mapped the distribution of two characters, which are here considered to be highly diagnostic in systematic and taxonomic discussions of Iguanodontia: the composition of the carpus (Fig. 9; Char. 91) and the number of sacral vertebrae, including dorsosacral and caudosacral ones (Fig. 10; Char. 185) on the strict consensus tree of the maximum parsimony.

The carpus is composed of unfused elements (Char. 91: 0) in neornithischians (e.g. *Hypsilophodon foxii*), early diverging iguanodontians (e.g. *Tenontosaurus tilletti*, *Dryosaurus altus*, *Dysalotosaurus lettowvorbecki*), and in the early diverging ankylopollexians (e.g. *Draconyx loureiroi*, *Uteodon aphanoecetes*). However, among the latter group, *Camptosaurus dispar* is the earliest taxon to show a carpus that is composed by several elements that are firmly interlocked into a solid structure (Char. 90: 1). This condition appears to be present in several different lineages of styracosternans and early diverging hadrosauroids. *Iguanodon bernissartensis* and *Magnamanus soriaensis* show a carpus formed by several carpal bones fused together to form a solid carpal unit (Char. 91: 2). *Tethyshadros insularis* and Hadrosauridae present a carpus composed by two small carpals (Char. 91: 3).

The count of sacral vertebrae is quite variable in the phylogeny: *Lesothosaurus diagnosticus* presents up to five sacral vertebrae (Char. 185: 0) while the earliest diverging members of Neornithischia and Iguanodontia show six sacral vertebrae (Char. 185: 1). This condition is retained by several taxa nested within Ankylopollexia and Styracosterna, however, several lineage-specific trends arise within the mentioned clades. For instance, *Uteodon aphanoecetes* reversed to the condition of having a count of five sacral vertebrae (Char. 185: 0), while *Bayannurosaurus perfectus*, *Ouranosaurus nigeriensis*, *Brighstoneus simmondsi* and *Mantellisaurus atherfieldensis* independently acquired a count of seven sacral vertebrae (Char. 185: 1). *Iguanodon bernissartensis* is the only non-hadrosaurid styracosternan to show a count of eight sacral vertebrae. Within Hadrosauroidea, the count ranges from six to seven, while eight or more sacral vertebrae is a synapomorphy of Hadrosauridae.

DISCUSSION

Systematic relationships of Iguanodontia

All phylogenetic analyses independent of the tree-searches strategies and character optimization criteria recover overall consistent consensus topologies, although there are some minor differences among them. These discrepancies were expected, since several other workers focusing on the phylogenetic relationships of Iguanodontia have remarked how unstable, and how sensitive to taxon and character sampling, these relationships are (McDonald 2012; Xu *et al.* 2018; Rozadilla *et al.* 2019, 2020; Lockwood *et al.* 2021; Poole 2022; Sánchez-Fenollosa *et al.* 2023).

One of the main shortcomings that these specialists have tried to overcome, is the inclusion of several previously neglected or overlooked European taxa within the general phylogenetic framework of the clade (Lockwood *et al.* 2021; Maidment *et al.* 2022; Rotatori *et al.* 2022; Bonsor *et al.* 2023; Sánchez-Fenollosa *et al.* 2023). Our dataset performed one additional step towards this direction, including for the first time several Late Jurassic to Early Cretaceous taxa from the Iberian Peninsula, a key palaeobiogeographical region due to its position close to Gondwanan and Mid-Atlantic plates (a classic 'dispersal' highway between Gondwanan and Laurasian plates; Krause *et al.* 2019).

The most notable result from our analysis is the recovery of a well-supported novel clade of high-sailed

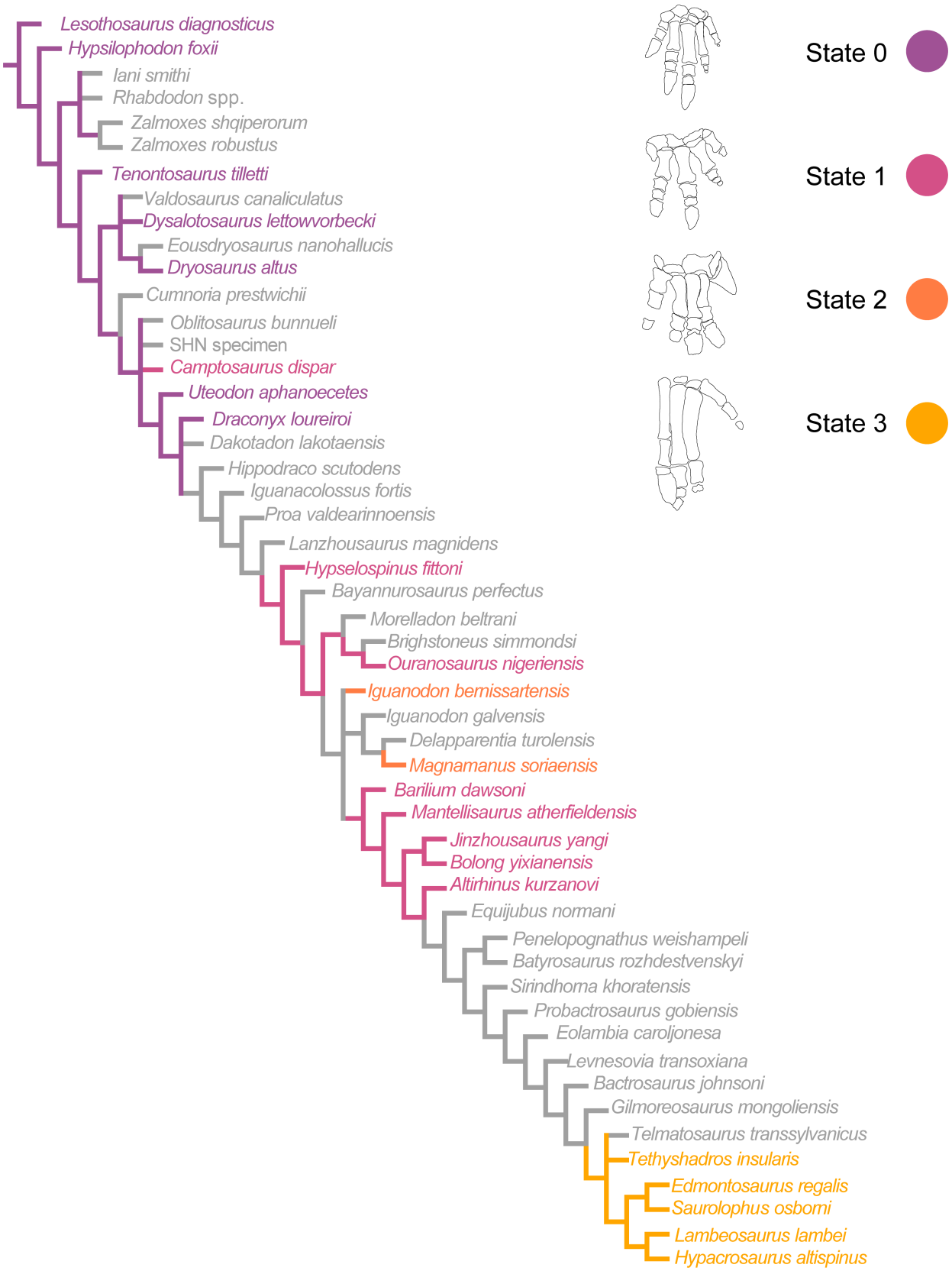

FIG. 9. Distribution of the character states of the carpal anatomy (Char. 91) within Iguanodontia mapped onto the strict consensus tree.

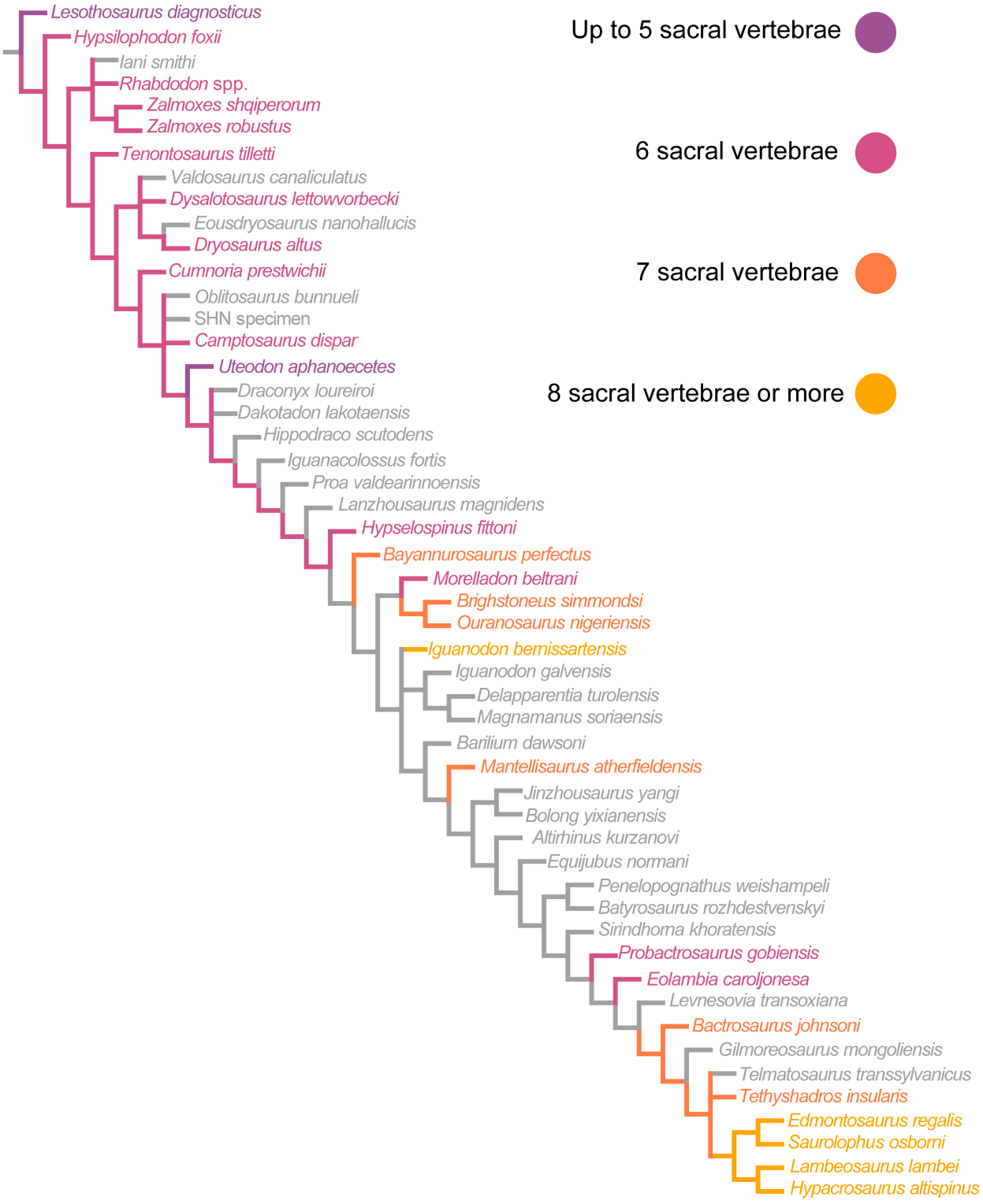

FIG. 10. Distribution of the number of sacral vertebrae (Char. 185) within Iguanodontia mapped onto the strict consensus tree.

Iguanodontians, Ouranosauria. Overall, the main distinguishing feature of this group is the presence of extremely high neural spines of the dorsal vertebrae, which groups together taxa from the early–mid Cretaceous of Europe and Africa. The sister clade relationship of *Brighstoneus simmondsi* and *Ouranosaurus nigeriensis* were first

recovered by Lockwood *et al.* (2021) in their 50% majority rule consensus tree. Several other lines of osteological evidence are presented in their work that possibly relate *Ouranosaurus nigeriensis* and *Brighstoneus simmondsi*, but see Lockwood *et al.* (2021) for details. Gasulla *et al.* (2015) recovered *Morelladon beltrani* as a hadrosauriform of dubious affinities in their analysis, although they noted several similarities between this taxon and *Ouranosaurus nigeriensis*. These similarities include the proportional height of neural spines of dorsal and sacral vertebrae compared to the height of their centra, shape and orientation of the preacetabular process of the ilium (Gasulla *et al.* 2015). In particular Gasulla *et al.* (2015, p. 11), stated that 'the neural spines of *Morelladon* resemble those of *Ouranosaurus nigeriensis* in being more anteroposteriorly expanded distally than proximally. However, the neural spines of *Ouranosaurus nigeriensis* are characterized by being extremely high (as much as 9 times centrum height)' and regarding the ilium: 'As in ... *Ouranosaurus nigeriensis*, the preacetabular process of the ilium in *Morelladon* is transversely compressed and oriented vertically, differing from the from the lateral torsion shown by *Barilium dawsoni* ...' (Gasulla *et al.* 2015, p. 19).

Furthermore, the morphology of the tibia bears another similarity between the two taxa recognized by Gasulla *et al.* (2015, p. 22): 'the tibia of *Morelladon* is very similar in morphology to those of *Mantellisaurus* and *Ouranosaurus* and more slender and lightly built than in *Iguanodon bernissartensis*'.

Accordingly, the recovery of a monophyletic Ouranosauria is consistent with all lines of evidence reported to date. We propose that a high-sailed, endemic clade of iguanodontian dinosaurs inhabited western Europe and Gondwana during the Early Cretaceous. The recently described *Istiorachis macarthurae* Lockwood *et al.* (2025), another styracosternan from the Isle of Wight, presents marked hyperelongation of the neural spines, similar in morphology and neural spine/centrum height ratio to *Morelladon beltrani* and *Ouranosaurus nigeriensis* (Lockwood *et al.* 2025). New analyses are needed to test for the inclusion of *Istiorachis macarthurae* within Ouranosauria, but we note that in the original phylogenetic analysis by Lockwood *et al.* (2025), which also used a modified version of Lockwood *et al.* (2021), they recovered *Istiorachis* as sister to *Ouranosaurus* (therefore by definition a member of this clade). Lockwood *et al.* (2025) discussed how the hyperelongation of the neural spines is a character most likely to be related to quadrupedality. Indeed, ouranosaurs and their peculiar structure appears in tandem with increased body-size (Chiarenza *et al.* 2021) and several osteological correlates to quadrupedal stance (Maidment & Barrett 2014; Lockwood *et al.* 2025). Future discoveries or a critical re-examination of key specimens will be required to test this hypothesis.

Taxonomic implications for the monophyly of Iguanodon

Our parsimony and Bayesian analyses consistently recover a paraphyletic *Iguanodon* grade: the Bernissart material traditionally referred to *Iguanodon bernissartensis* forms a lineage separate from an Iberian Barremian clade comprising '*Iguanodon*' *galvensis*, *Delapparentia turolensis* and *Magnamanus soriaensis*. From an alpha-taxonomic perspective, such paraphyly requires a narrowing of *Iguanodon* to a diagnosable, monophyletic unit anchored on the Bernissart hypodigm, and reallocating Iberian species that demonstrably fall outside that lineage. We therefore treat *Iguanodon* sensu stricto (s.s.) as the *I. bernissartensis* lineage only and regard the Iberian Barremian forms as members of Iguanodontidae (*sensu* Madzia *et al.* 2021) outside the genus *Iguanodon*. In both the implied weighting *k*9–12 analyses (Fig. S4) and the tip-dated Bayesian analysis (Fig. 4), *I. bernissartensis* plus Iberian styracosternans are recovered within Iguanodontidae, as previously defined by Verdú *et al.* (2015, 2017a), since '*Iguanodon*' *galvensis* is recovered in all the analyses as more closely related to the clade formed by *Magnamanus soriaensis* + *Delapparentia turolensis*, than to *Iguanodon bernissartensis*.

Delapparentia turolensis was erected by Ruiz-Omeñaca (2011), and its affinities were better discussed by Gasca *et al.* (2015). Later works considered this species to be a *nomen dubium* (Norman 2015, Verdú *et al.* 2017a), suggesting that it could be considered as a junior synonym of *Iguanodon bernissartensis*. However, several features are incongruent with the referral to *Iguanodon bernissartensis*. As reconstructed by Gasca *et al.* (2015), the shape of the preserved prepubic process in *Delapparentia turolensis*, falls outside the intraspecific variability documented for *Iguanodon bernissartensis*: the pubic shaft shows strongly concave/convex dorsal and ventral margins and a cranial apex projecting dorsocranially (Verdú *et al.* 2017b), a condition closer to that observed in *Lurdusaurus arenatus* (Taquet & Russell 1999). Direct comparison of the iliac blade with *Iguanodon bernissartensis* is complicated by documented taphonomic distortion in the Bernissart sample (Verdú *et al.* 2017b; see also Norman 2012): the preacetabular process ranges from being strongly ventrally deflected to sub-horizontal. However, as stated by Verdú *et al.* (2017b): 'most of the *I. bernissartensis* specimens from Bernissart have distorted ilia, but the dorsal margin of the ilium is only slightly convex and nearly straight in specimens with roughly undistorted dorsal margins, such as RBINS R51, RBINS R341, and RBINS R352, as previously described by Norman (2012)'. In this regard, the dorsal blade of the ilium of *Delapparentia turolensis* falls within the range of variation reported by the authors.

By contrast, the Barremian clade from Iberia is supported by consistent mandibular and pelvic morphologies.

Two dentary characters diagnose this grouping: a coronoid process that is set approximately perpendicular to the dorsal margin of the dentary (Char. 52: 1) and whose apex is suboval and anteroposteriorly expanded (Char. 53: 0). Because '*I.*' *galvensis* lacks the eight-sacral count autapomorphic of *Iguanodon* s.s. and shows the Iberian mandibular morphology, its retention within *Iguanodon* would perpetuate paraphyly. We therefore remove '*I.*' *galvensis* from *Iguanodon* and regard it as requiring a new generic name within Iguanodontidae, to be accompanied by a formal differential diagnosis against *I. bernissartensis*, *Delapparentia* and *Magnamanus*.

Delapparentia turolensis and *Magnamanus soriaensis* share as unambiguous synapomorphy a mediolaterally compressed, dorsoventrally narrow and parallel-sided prepubic process (Char. 106: 2). This condition is different from both '*Iguanodon*' *galvensis* and *Iguanodon bernissartensis* which present almost identical prepubic process, indeed a mediolaterally compressed, and deeply expanded dorsoventrally in the distal region (Char. 106: 3). The character causing the nesting of *Delapparentia turolensis* and *Magnamanus soriaensis* in a clade alongside with '*Iguanodon*' *galvensis*, is the coronoid process of dentary perpendicular to the dorsal edge of the dentary ramus (Char. 52: 0>1) and its finger-like apical shape (Char. 53: 1>0).

A re-diagnosis of *Iguanodon* s.s. is best built around features that: (1) overlap with frequently preserved elements; and (2) show minimal homoplasy in our matrices. The most reliable autapomorphy we recover for *I. bernissartensis* among non-hadrosaurid styracosternans is a sacral count of eight vertebrae (Char. 185), a condition otherwise restricted to Hadrosauridae in our sample. We pair this with a compound character set that should not be used individually but, in combination, strengthening referrals when the sacrum is incomplete: (1) fused carpus forming a single unit (Char. 91: 2); and (2) a prepubic process that is mediolaterally compressed and deeply expanded distally (Char. 106: 3). Equally important are exclusionary criteria: *Iguanodon* s.s. lacks the axial 'high-sail' complex that defines the Ouranosauria clade in our trees (very tall dorsal neural spines; neural spine centred over the dorsal centrum; strongly caudodorsal post-acetabular rim: chars 129, 140, 150). On present evidence, we recommend that no specimen be referred to *Iguanodon* s.s. without either: (1) a preserved eight-sacral series; or (2) the carpus-plus-pubis combination above together with absence of Ouranosauria-like axial features and a compatible overall morphology. The character-state maps for sacral counts (Fig. 10) and carpal composition (Fig. 9) emphasize why such compound diagnoses are necessary: both regions show repeated convergence.

While a deep taxonomic revision of the Iberian styracosternan iguanodontians being beyond the scope of this paper, we have presented here evidence that the Iberian styracosternan dinosaurs dated to the Early Cretaceous are closely related to one another, and the attribution of the Iberian material to *Iguanodon bernissartensis* seems unlikely. Furthermore, as indicated by the character states maps of the count of the sacral vertebrae (Fig. 10) and the carpal bones composition (Fig. 9), the postcranial skeleton is highly plastic and prone to homoplasy. Therefore, identification to species level of very fragmentary remains is potentially misleading (Gasulla *et al.* 2022). In the implied weighting $k = 9$ to $k = 11$ analyses (Figs S11–S13) and the tip dated Bayesian inference analysis (Fig. 6) *Iguanodon bernissartensis* + Iberian styracosternans are recovered within the clade Iguanodontidae (*sensu* Madzia *et al.* 2021). This clade ranges from early to late Barremian of Europe and it is likely that the diversity we observe is a result of complex macroevolutionary events occurring in the Iberian plate and areas corresponding to the Wealden facies. The recovery of a distinct sub-clade of Iberian styracosternans is comparable in diversity to the assemblages in other part of Western Europe. As we see in the UK, both in the Hastings Basin and Isle of Wight, there is a high diversity of hadrosauriform styracosternans in the same formations (Norman 2011, 2015; Lockwood *et al.* 2021, 2024, 2025; Bonsor *et al.* 2023) even though different species are likely to have been separated by several millions of years (see the recent work on Isle of Wight iguanodontians: Lockwood *et al.* 2021, 2024, 2025). A complex interplay of anagenetic and cladogenetic events may have produced the observed diversity. Furthermore, the British fauna appear to have been more distinctive than previously thought; for example, the attribution of robust specimens to *Iguanodon bernissartensis* has been re-evaluated (Lockwood *et al.* 2024). This segregation of faunas is further supported by the fact that Early Cretaceous styracosternans seem to have been non-migratory species, prone to inhabiting restricted geographic areas (Decrée *et al.* 2026). It is therefore not surprising that a distinct, peculiar assemblage has been discovered in Iberia (Chiarenza et al. 2021). *Magnamanus soriaensis*, *Delapparentia turolensis* and '*Iguanodon*' *galvensis* are early Barremian in age, while *Morelladon beltrani*, specimens attributed either to *Mantellisaurus atherfieldensis* or *Iguanodon bernissartensis* and the intriguing Barranco del Hocino taxon are dated to the late Barremian (Medrano-Aguado *et al.* 2023). This temporal segregation, much better documented than the one occurring on the Isle of Wight, lead us hypothesize that even in this case a mixture of anagenetic and cladogenetic events produced such diversity. The recent identification of the putative hadrosauroid *Cariocecus bocagei* Bertozzo *et al.* (2025) from the Lower Cretaceous of Portugal, further supports the interpretation of the British and Iberian assemblages as distinct macro regions. Reappraisal of the historical

specimens is needed to further enhance the resolution of the inter-relationships of this clade. Therefore, we regard the attribution of isolated material to *Iguanodon bernissartensis* or *Mantellisaurus atherfieldensis* recovered from the Iberian Peninsula as dubious (Gasulla *et al.* 2022; Berrocal-Casero *et al.* 2025).

Morphological evolutionary trends within Iguanodontia. We mapped the distribution of two characters: the composition of the carpus (Char. 91; Fig. 9) and number of the sacral vertebrae (Char. 185; Fig. 10). As mentioned above, character 91 is related to the composition of the carpus, and states from 0 to 3 describe a more progressively rigid, less prone to grasping unit. In general, these features are related to the acquisition of quadrupedal stance (Maidment & Barrett 2014). We observe that early diverging iguanodontians and some ankylopollexians, such as *Draconyx loureiroi* or *Uteodon aphanoecetes* (Carpenter & Wilson 2008; Rotatori *et al.* 2022), present non-interlocked carpal bones and relatively elongated metacarpals suggesting the presence of grasping function for the hand (Fig. S15). *Camptosaurus dispar*, presents interlocked but not fused carpal bones and less elongated, more robust metacarpals, suggesting a shift towards quadrupedality as indicated by Maidment & Barrett (2014). Styracosternans further developed carpal fusion towards graviportality as mirrored in other graviportal amniotes (Harrison & Manning 1983; Läng & Goussard 2007): *Magnamanus soriaensis* and *Iguanodon bernissartensis* developed totally fused carpals bones (Char. 91: 3) forming a rigid structure, while other taxa such as *Mantellisaurus atherfieldensis*, *Ouranosaurus nigeriensis*, and some early diverging hadrosaurids retained multiple carpals not totally fused (Char. 91: 2) (Fig. S15). Both groups have relatively robust, compressed metacarpals, characters strongly correlated to quadrupedality (Maidment & Barrett 2014).

The differences in the anatomy of the carpus of different iguanodontian, putatively quadrupedal lineages may indicate that: (1) each lineage probably achieved a quadrupedal lifestyle; and (2) the function of the hypertrophied ungual pollex ('swiss-knife hand') of some hadrosauriform may have served to multiple uses.

If we evaluate the distribution of the number of sacral vertebrae (Char. 185) we see a similar pattern: earlier diverging forms have generally fewer sacral vertebrae, while styracosternans, including hadrosauroids show a wide variation in the sacral count. Although we do not exclude potential preservational bias with this model, as shown in data variability from hadrosauriforms (Lockwood *et al.* 2021), we regard this general trend to be genuine. The number of sacral vertebrae is related to the development of the iliac blade, which is a pivotal site for muscle attachments functional to locomotion (Barrett & Maidment 2017). Again, changes in size and morphology of the iliac blade are key shifts in ornithischians attainment of quadrupedality (Maidment & Barrett 2014). Therefore, this variation in number of sacral vertebrae may reflect different quadrupedal locomotion styles in Styracosterna.

Our expanded postcranial sampling underscores that several historically popular characters for diagnoses are highly homoplastic or taphonomically labile, and should be down-weighted unless they co-occur as part of a broader pattern. Notably, the fused-unit state (Char. 91: 2) occurs in *I. bernissartensis* but also in *Magnamanus*, so it is likely to be symplesiomorphic and supportive only in combination with other features. Sacral counts of six or seven recur independently (e.g. *Bayannurosaurus*, *Ouranosaurus*, *Brighstoneus*, *Mantellisaurus*), whereas a count of eight sacrals appears as a unique outlier in the *I. bernissartensis* lineage outside hadrosaurids; counts below eight therefore have limited diagnostic value. In general, given the high plastic nature of this character, we again recommend caution when identifying fragmentary material based solely on the count of sacral vertebrae. Femoral shaft curvature (Char. 115) and several iliac characters (preacetabular twist and dorsal-margin thickening/eversion: Chars 100, 102, 152) shift state assignments between parsimony and Bayesian optimizations and are especially susceptible to distortion. Similarly, axial features used to define Ouranosauria (Chars 129, 140, 150) are excellent for excluding *Iguanodon* s.s. but can be obscured or accentuated by preservation; caudal traits (ventral sulcus, chevron-facet proportions: Chars 191, 198) are also highly homoplastic across Dryomorpha/Styracosterna.

These new observations, together with the hypothesized role of hypertrophic neural spines in quadrupedal locomotion (Lockwood *et al.* 2025), suggest two implications. First, the Early Cretaceous was not only a hotspot of alpha diversity in styracosternan iguanodontians, but also a peak of locomotor disparity, during which multiple lineages experimented with distinct quadrupedal stances. One pathway involved increasing the sacral vertebral count to support enlarged iliac blades (taken to an extreme in the *Iguanodon bernissartensis* lineage) whereas another, centred on hyperelongation of the dorsal neural spines, developed in Ouranosauria. These trends probably reflect a complex functional and developmental interplay. Second, among these alternatives, the hadrosauroid condition (encompassing carpal architecture, neural-spine proportions, and sacral count) ultimately became predominant over other later diverging, iguanodontian bauplans.

Origin of Iguanodontia & its historical biogeography. The first attempt to include neglected European taxa within

detailed iguanodontian biogeographical history and macroevolutionary reconstruction provided a solid framework to infer the early stages of the distribution of the clade, and had important implications for its systematics. From a chronological perspective, the fossil record assigned to Iguanodontia is dated to the Middle Jurassic (Callovian; Ruiz-Omeñaca *et al.* 2006), although recent discoveries indicate the presence of cerapodan dinosaurs (Maidment *et al.* 2025) in the Bathonian of Africa, and even the possible presence of iguanodontians in coeval deposits of Europe (Panciroli *et al.* 2025). Iguanodontian dinosaurs are possibly sampled in coeval deposits of northwestern Europe (Panciroli *et al.* 2025). The authors of the latter study stated that 'although the highly fragmentary state of NMS G.2023.19.1 precludes definitive identification, we suggest that the specimen represents a basal cerapodan or ornithopod, and perhaps even an iguanodontian, given its size and similarity to *Cumnoria*' (Panciroli *et al.* 2025 p. 10). Of further interest, dePolo *et al.* (2020) described a series of exceptionally large ornithopod footprints from the Bajocian–Bathonian (*c.* 170–166 Ma) of the Isle of Skye (Scotland, UK) and hypothesized that the trackmaker was a *Camptosaurus*-like ankylopollexian. These authors explicitly stated that 'the ornithopod tracks found on Skye could have been made by a smaller, primitive member of the generally large-bodied ankylopollexian clade–a ghost taxon, unrecorded by body fossils, known only from its traces. In summary, we suggest that the trackmaker for Skye's large ornithopod tracks (if, indeed, the tridactyl footprints at BP3 and GLAHM V1980 are such) belongs to the clade Dryomorpha (the Dryosauridae + Ankylopollexian clade). It could either be a larger member of Dryosauridae or, alternatively, a small, basal ankylopollexian. In general, 'ornithopod'-type footprints from the Early–Middle Jurassic are small (12–20 cm) with some compelling medium to large prints known from Yorkshire. The ornithopod tracks found on Skye are some of the earliest potential large ornithopod footprints known from anywhere in the world, providing additional evidence for the existence of fairly large-bodied ornithopods in the Middle Jurassic and augmenting the sparse body fossil record for this time interval.' (dePolo *et al.* 2020 p. 40). If the ankylopollexians had already diversified by the Bajocian–Bathonian, we could infer an extensive ghost lineage of early-diverging iguanodontian branches.

Some caveats may arise when considering the discrepancies between different models since the FBD models produced here recover more 'orthodox' divergence times for most of the clades. However, as discussed above, we note that the early radiation of Iguanodontia is not yet clearly spatiotemporally constrained and that some evidence points out to older origins (dePolo *et al.* 2020; Maidment *et al.* 2025; Panciroli *et al.* 2025). Therefore, we explicitly state this is a hypothesis worth exploring, whose scenario and implications are discussed hereafter. The historical biogeographic reconstruction under this heterodox hypothesis, therefore, neither supports nor is reconcilable with other recent phylogenetic and biogeographic analyses on Iguanodontia (i.e. Xu *et al.* 2018; Poole 2022; Bertozzo *et al.* 2025).

In terms of geographic patterns, the early evolution and radiation events of Iguanodontia is nested within Europe and North America (see also Xu *et al.* 2018) and this study discriminates dispersal events between North America and Europe in the Middle Jurassic. The origin of Iguanodontia is recovered from the analysis in the Pliensbachian, 16 million years earlier than the ichnological evidence of putative ankylopollexian dinosaurs would indicate (dePolo *et al.* 2020). At that time, the global scenario was marked by major biotic turnover, global climatic changes, and continental fragmentation where Europe was a set of islands located in the western Tethys (Upchurch & Chiarenza 2024). Furthermore, late Pliensbachian black shales have been suggested to record a climatic hyperthermal event (Thierry 2000; Dera *et al.* 2010; Silva & Duarte 2015; Ruhl *et al.* 2016; Bougeault *et al.* 2017; Ruebsam & Al-Husseini 2020; Schöllhorn *et al.* 2020). Interestingly, this episode coincided with detectable macroevolutionary trends (Chiarenza *et al.* 2024), acceleration in evolutionary rates (Fig. 6), and dispersal to North America of dryosaurids, ankylopollexians and styracosternans by the Toarcian–Aalenian (Figs 2, 4). Emerged areas in the European region during the Early Jurassic were reduced (Silva *et al.* 2021), vast insular systems located between major landmasses (Upchurch & Chiarenza 2024) and hyperthermal conditions may have fostered occasional dispersal routes, population fragmentation and therefore triggered higher rates of speciation as found by other studies (Lloyd *et al.* 2008; Olsen *et al.* 2022; Dunne *et al.* 2023). In this context, oceanic dispersal as proposed for later diverging hadrosaurids may also have been a viable mechanism (Longrich *et al.* 2021).

The radiation of several lineages of iguanodontians by the late Toarcian (Figs 2, 4) parallels what is seen in tetanuran theropods (Rauhut *et al.* 2015, 2016; Rauhut & Pol 2019). Well documented climatic shifts during the Toarcian resulted in several extinction pulses during the late Pliensbachian, which Rauhut *et al.* (2016) related to the increase in diversity of theropod dinosaurs as consequence of the Toarcian Anoxic Event. This event is linked with massive volcanic activity of the Karoo–Ferrar region, which produced several extinction pulses during the late Pliensbachian (Wignall 2001). Besides theropod dinosaurs, this event is believed to have sparked radiation in other groups (Close *et al.* 2015; Chiarenza *et al.* 2024), and more importantly to the other main dinosaurian

primary consumer groups, eusauropods (Pol *et al.* 2020). Despite the lack of direct fossil evidence, our analysis concurs that these events may have also played a role in the early diversification of Iguanodontia.

Furthermore, our analysis highlights that all the major clades of iguanodontians, evolved and dispersed globally by the end of the Late Jurassic. We speculate that large sized, earlier diverging Iguanodontiforms, including Iguanodontidae and the herein newly recovered Ouranosauria, might have originated in this spatiotemporal context, the Middle–Late Jurassic interval between Europe and North America, with a later dispersal to Gondwana via western European microplates between the latest Jurassic and earliest Cretaceous. Hadrosauroidea is the main iguanodontian clade to have dispersed into Asia, where this clade subsequently diversified after the Jurassic–Cretaceous transition. This is in agreement with a global distribution and lack of segregation of faunas during the Late Jurassic (Ezcurra & Agnolín 2012; Fanti 2012), which did not happen before the rifting phases due to the fragmentation of Gondwanan landmasses during the Early Cretaceous (Krause *et al.* 2019). The heterogeneous composition of the several iguanodontian faunas dated to the Early Cretaceous respectively from Europe, Asia and North America is here attributed to local extinction events. This is particularly evident from the absence of non-hadrosauroid iguanodontians in Asia after the Aptian, although their presence is registered in the continent by at least two taxa (Xu *et al.* 2018), an interpretation here corroborated by both DIVALIKE + j and the DEC + j model results of our analysis. Hadrosauroidea is the only lineage of Styracosterna that survived into the Late Cretaceous, indicating the presence of a prominent turnover, probably happening at the Early–Late Cretaceous transition (possibly related to the Cretaceous Thermal Maximum; Zanno *et al.* 2019, 2023; Chiarenza *et al.* 2024).

As supported by data presented here, Europe experienced faunal isolation from the Barremian to the early Albian (Ezcurra & Agnolín 2012) probably due to sea-level high stand (Csiki-Sava *et al.* 2015). This is supported by our analysis which produces a hadrosauroid dispersal in North America by the Aptian–Albian (Fig. 8), and an immigration into Europe from Asia in the Late Cretaceous, before the Campanian, with the node including *Tethyshadros insularis* + *Telmatosaurus transylvanicus* (Grigorescu & Csiki 2006; Chiarenza *et al.* 2021). Other clades both from Gondwana and Asia immigrated in Europe by that time, indicating the end of the isolation in the continent probably due to tectonically controlled land emersion during the earliest Late Cretaceous (Fanti 2012; Conti *et al.* 2020; Randazzo *et al.* 2021; Vila *et al.* 2022; Muscioni *et al.* 2023). These results highlight the pivotal role of western European plates in the early dispersal and diversification of Iguanodontia, as previously suggested by other authors (Xu *et al.* 2018; Rotatori *et al.* 2020, 2022, 2025; Sánchez-Fenollosa *et al.* 2023).

CONCLUSIONS

We have assembled a new dataset matrix comprising most of the iguanodontian dinosaur taxa currently known, with a strong emphasis on neglected European taxa. We performed a series of phylogenetic analyses, employing both maximum parsimony and Bayesian inference. The tip-dated tree was used to reconstruct the biogeographic history of the clade. The main findings of this study include:

1. The identification of a new clade of dinosaurs, named Ouranosauria, which comprises high-sailed styracosternans from the Early Cretaceous.
2. The recovery of a paraphyletic *Iguanodon* genus as previously defined by other workers, indicating the close relationships of Iberian styracosternans recovered in the Barremian and suggesting the absence of *Iguanodon bernissartensis* in Southern Europe.
3. The time calibrated phylogeny indicates overall constant evolutionary rates, with most iguanodontian clades originating before the Jurassic-Cretaceous boundary.
4. Iguanodontian originated and diversified in Laurasia over 186 million years ago and attained global distribution before the Jurassic–Cretaceous transition in different pulses via dispersal, vicariance, cladogenetic and jump dispersal events. The heterogeneous faunal composition we observe during the Early Cretaceous among Asia, Europe and North America might be explained in terms of local extinction events.
5. Character mapping reveals a mosaic of traits associated with quadrupedality and increased body-size that emerged alongside the radiation of Early Cretaceous styracosternans. This remarkable bauplan disparity suggests a comparable high diversity of locomotor strategies within this group.

Acknowledgements. We would like to thank several institutions in which we collected several first-hand observations on the specimens and species discussed here. In particular Susannah Maidment from Natural History Museum (London) who also provided valuable comments on a first draft of the manuscript, Hillary Ketchum (Oxford University Museum of Natural History), Martin Munt (Dinosaur Isle Museum, Isle of Wight), Deborah Arbulla (Museo Civico Storia Naturale Trieste) and Sanjaadash Ulziitseren for access to the collections at the Institute of Palaeontology of the Mongolian Academy of Sciences. We thank Carl Mehling from American Museum of Natural History (New York) for hosting and taking great care of FMR during his collection visit. We thank also Manuel Peréz and Eduardo Medrano-Aguado

for their help during FMR's collection visit to Spain. We further thank all the staff of the following museums for assistance: Yale Peabody Museum, Carnegie Museum, Field Museum, Stuttgart Museum of Natural History, Geological and Paleontological Institute of Tubingen, Museo Numantino de Soria, Fundacion Dinópolis-Teruel, Museo Aragones de Paleontología and Herrero Museum. We thank Sara Varela (Vigo University) and the whole MAPAS Lab to have hosted and trained FMR during his PhD internship. This work was supported by the National Funds through the FCT – Fundação para a Ciencia e a Tecnologia, I.P., through the Research Unit UIDB/04035/2020, the Project PTDC/CTA-PAL/2217/2021, SFRH/BD/146230/2019 (FMR) and COVID/BD/153554/2024 (FMR). FMR benefited from the ERASMUS+ program and a Jurassic Foundation Grant. MMA is supported by the MCIN/AEI/10.13039/501100011033 and co-financed by the NextGeneration EU/PRTR, Ramón y Cajal contract RYC2021-034473-I and Ministerio de Ciencia e Innovación with the grant PID2021-122612OB-100 and the project PID2024-158833OB-I00. AAC was funded by a Newton International Fellowship from The Royal Society (grant NIF\R1\231802), a European Research Council (ERC) Starting Grant under the European Union's Horizon 2020 Research and Innovation Programme (grant 947921 'Mapas' to Sara Varela) and by a Juan de la Cierva Formación 2020 Fellowship (grant FJC2020-044836-I) from the Ministry of Science and Innovation and the European Union Next Generation EU/PRTR. We thank Terry A. Gates, an anonymous reviewer, and the editors David Button and Sally Thomas whose comments greatly improved the quality of this manuscript.

Author contributions. **Conceptualization** Filippo Maria Rotatori (FMR), Alfio Alessandro Chiarenza (AAC), Federico Fanti (FF), Miguel Moreno-Azanza (MMA); **Data Curation** FMR; **Formal Analysis** FMR, AAC, MMA; **Funding Acquisition** FMR, MMA; **Investigation** FMR; **Methodology** FMR, AAC; **Project Administration** MMA; **Resources** AAC, MMA; **Software** FMR, MMA, AAC; **Supervision** AAC, FF, MMA; **Validation** AAC, FF, MMA; **Visualization** FMR, AAC; **Writing – Original Draft Preparation** FMR, AAC; **Writing – Review & Editing** FMR, AAC, FF, MMA.

DATA ARCHIVING STATEMENT

Supporting information and datasets of this manuscript necessary to replicate phylogenetic and biogeographical analyses are archived in MorphoBank: https://www.morphobank.org/permalink/?P5992 (including: the general matrix used for this contribution, .tnt ready file to be used accordingly to the scripts provided, NEXUS files to replicate the analyses, BioGeoBears script, tip-dated MCT, dispersion matrix and distribution data).

This published work has been registered in ZooBank: https://zoobank.org/references/A0FDE1E7-4BD6-4DA4-893A-C602FEAE3827.

Editor. David Button

SUPPORTING INFORMATION

Additional Supporting Information can be found online (https://doi.org/10.1111/pala.70057):

Appendix S1. Supplementary information on sensitivity tests. Includes: Figs S1–S4 (trees from sensitivity tests); Figs S5–S13 (strict consensus trees from implied weight analyses ($k = 3$ to $k = 11$)); Fig. S14 (maximum compatibility tree of the non-clock Bayesian inference analysis); and Fig. S15 (morphological trends within the carpus of Iguanodontia).

REFERENCES

Alarcón-Muñoz, J., Vargas, A. O., Püschel, H. P., Soto-Acuña, S., Manríquez, L., Leppe, M., Kaluza, J., Milla, V., Gutstein, C. S., Palma-Liberona, J., Stinnesbeck, W., Frey, E., Pino, J. P., Bajor, D., Núñez, E., Ortiz, H., Rubilar-Rogers, D. and Cruzado-Caballero, P. 2023. Relict duck-billed dinosaurs survived into the last age of the dinosaurs in subantarctic Chile. *Science Advances*, **9**, eadg2456.

Allain, R., Vullo, R., Rozada, L., Anquetin, J., Bourgeais, R., Goedert, J., Lasseron, M., Martin, J. E., Pérez-García, A. and de Fabrègues, C. P. 2022. Vertebrate paleobiodiversity of the Early Cretaceous (Berriasian) Angeac-Charente Lagerstätte (southwestern France): implications for continental faunal turnover at the J/K boundary. *Geodiversitas*, **44**, 683–752.

Baron, M. G. 2019. *Pisanosaurus mertii* and the Triassic ornithischian crisis: could phylogeny offer a solution? *Historical Biology*, **31**, 967–981.

Barrett, P. M. and Maidment, S. C. 2017. The evolution of ornithischian quadrupedality. *Journal of Iberian Geology*, **43**, 363–377.

Barrett, P. M. and Maidment, S. C. 2025. A review of *Nanosaurus agilis* Marsh and other small-bodied Morrison Formation "ornithopods". *Bulletin of the Peabody Museum of Natural History*, **66**, 25–50.

Bell, P. R., Herne, M. C., Brougham, T. and Smith, E. T. 2018. Ornithopod diversity in the Griman Creek Formation (Cenomanian), New South Wales, Australia. *PeerJ*, **6**, e6008.

Berrocal-Casero, M., Barroso-Barcenilla, F., Callapez, P. M., Pimentel, R., Alcalde-Fuentes, M. R. and Prieto, I. 2025. New ornithopod remains from the upper Barremian (Lower Cretaceous) of Vadillos-1 (Cuenca, Spain). *Fossil Studies*, **3**, 5.

Bertozzo, F., Camilo, B., Araújo, R., Manucci, F., Kullberg, J. C., Cerio, D. G., de Carvalho, V. F., Marrecas, P., Figueiredo, S. D. and Godefroit, P. 2025. *Cariocecus bocagei*, a new basal hadrosauroid from the Lower Cretaceous of Portugal. *Journal of Systematic Palaeontology*, **23**, 2536347.

Bonsor, J. A., Lockwood, J. A. F., Leite, J. V., Scott-Murray, A. and Maidment, S. C. R. 2023. The osteology of the holotype of the British iguanodontian dinosaur *Mantellisaurus atherfieldensis*. *Monographs of the Palaeontographical Society*, **177**, 1–63.

Bougeault, C., Pellenard, P., Deconinck, J.-F., Hesselbo, S. P., Dommergues, J.-L., Bruneau, L., Cocquerez, T., Laffont, R., Huret, E. and Thibault, N. 2017. Climatic and

palaeoceanographic changes during the Pliensbachian (Early Jurassic) inferred from clay mineralogy and stable isotope (C-O) geochemistry (NW Europe). *Global and Planetary Change*, **149**, 139–152.

Boulenger, G. A. 1881. Sur l'arc pelvien chez les dinosauriens de Bernissart [On the pelvic arch in the dinosaurs of Bernissart]. *Bulletins de L'Académie royale de Belgique, 3eme série*, **1** (5), 1–11.

Boyd, C. A. 2015. The systematic relationships and biogeographic history of ornithischian dinosaurs. *PeerJ*, **3**, e1523.

Brown, E. E., Butler, R. J., Barrett, P. M. and Maidment, S. C. 2021. Assessing conflict between early neornithischian tree topologies. *Journal of Systematic Palaeontology*, **19**, 1183–1206.

Burnham, K. P. and Anderson, D. R. 2002. *Model selection and multimodel inference: A practical information-theoretic approach*. Springer.

Butler, R. J., Upchurch, P. and Norman, D. B. 2008. The phylogeny of the ornithischian dinosaurs. *Journal of Systematic Palaeontology*, **6**, 1–40.

Carpenter, K. and Galton, P. M. 2018. A photo documentation of bipedal ornithischian dinosaurs from the Upper Jurassic Morrison Formation, USA. *Geology of the Intermountain West*, **5**, 167–207.

Carpenter, K. and Lamanna, M. C. 2015. The braincase assigned to the ornithopod dinosaur *Uteodon* McDonald, 2011, reassigned to *Dryosaurus* Marsh, 1894: implications for iguanodontian morphology and taxonomy. *Annals of Carnegie Museum*, **83**, 149–166.

Carpenter, K. and Wilson, Y. 2008. A new species of *Camptosaurus* (Ornithopoda: Dinosauria) from the Morrison Formation (Upper Jurassic) of Dinosaur National Monument, Utah, and a biomechanical analysis of its forelimb. *Annals of Carnegie Museum*, **76**, 227–264.

Chiarenza, A. A., Cantalapiedra, J. L., Jones, L. A., Gamboa, S., Galván, S., Farnsworth, A. J., Valdes, P. J., Sotelo, G. and Varela, S. 2024. Early Jurassic origin of avian endothermy and thermophysiological diversity in dinosaurs. *Current Biology*, **34**, 2517–2527.e4.

Chiarenza, A. A., Fabbri, M., Consorti, L., Muscioni, M., Evans, D. C., Cantalapiedra, J. L. and Fanti, F. 2021. An Italian dinosaur Lagerstätte reveals the tempo and mode of hadrosauriform body size evolution. *Scientific Reports*, **11**, 1–15.

Chiarenza, A. A., Mannion, P. D., Farnsworth, A., Carrano, M. T. and Varela, S. 2022. Climatic constraints on the biogeographic history of Mesozoic dinosaurs. *Current Biology*, **32**, 570–585.e3.

Close, R. A., Friedman, M., Lloyd, G. T. and Benson, R. B. 2015. Evidence for a mid-Jurassic adaptive radiation in mammals. *Current Biology*, **25**, 2137–2142.

Conti, S., Vila, B., Sellés, A. G., Galobart, À., Benton, M. J. and Prieto-Márquez, A. 2020. The oldest lambeosaurine dinosaur from Europe: insights into the arrival of Tsintaosaurini. *Cretaceous Research*, **107**, 104286.

Crisp, M. D., Hardy, N. B. and Cook, L. G. 2014. Clock model makes a large difference to age estimates of long-stemmed clades with no internal calibration: a test using Australian grasstrees. *BMC Evolutionary Biology*, **14**, 263.

Cruzado-Caballero, P., Gasca, J. M., Filippi, L. S., Cerda, I. A. and Garrido, A. C. 2019. A new ornithopod dinosaur from the Santonian of Northern Patagonia (Rincón de los Sauces, Argentina). *Cretaceous Research*, **98**, 211–229.

Csiki-Sava, Z., Buffetaut, E., Ősi, A., Pereda-Suberbiola, X. and Brusatte, S. L. 2015. Island life in the Cretaceous – faunal composition, biogeography, evolution, and extinction of land-living vertebrates on the Late Cretaceous European archipelago. *ZooKeys*, **469**, 1–161.

Decrée, S., Leduc, T., Godefroit, P., Deloule, E., Coint, N., Huyskens, M. H., Mansur, E. T., Debaille, V. and Baele, J.-M. 2026. Analysis of *Iguanodon bernissartensis* teeth and bones using in-situ trace element, oxygen and strontium isotope composition: Implication for paleoecology, paleoenvironment and diagenesis. *Palaeogeography, Palaeoclimatology, Palaeoecology*, **681**, 113371.

dePolo, P. E., Brusatte, S. L., Challands, T. J., Foffa, D., Wilkinson, M., Clark, N. D., Hoad, J., Pereira, P. V. L. G. d. C., Ross, D. A. and Wade, T. J. 2020. Novel track morphotypes from new tracksites indicate increased Middle Jurassic dinosaur diversity on the Isle of Skye, Scotland. *PLoS One*, **15**, e0229640.

Dera, G., Neige, P., Dommergues, J.-L., Fara, E., Laffont, R. and Pellenard, P. 2010. High-resolution dynamics of Early Jurassic marine extinctions: the case of Pliensbachian–Toarcian ammonites (Cephalopoda). *Journal of the Geological Society*, **167**, 21–33.

Dieudonné, P.-E., Cruzado-Caballero, P., Godefroit, P. and Tortosa, T. 2020. A new phylogeny of cerapodan dinosaurs. *Historical Biology*, **33**, 1–21.

dos Reis, M., Donoghue, P. C. J. and Yang, Z. 2016. Bayesian molecular clock dating of species divergences in the genomics era. *Nature Reviews Genetics*, **17**, 71–80.

Dunne, E. M., Farnsworth, A., Benson, R. B. J., Godoy, P. L., Greene, S. E., Valdes, P. J., Lunt, D. J. and Butler, R. J. 2023. Climatic controls on the ecological ascendancy of dinosaurs. *Current Biology*, **33**, 206–214.e4.

Edgar, K. M., Haller, L., Cashmore, D. D., Dunne, E. M. and Butler, R. J. 2023. Stratigraphic and geographic distribution of dinosaur tracks in the UK. *Journal of the Geological Society*, **180**, jgs2023-003.

Escaso, F., Ortega, F., Dantas, P., Malafaia, E., Silva, B., Gasulla, J. M., Mocho, P., Narváez, I. and Sanz, J. L. 2014. A new dryosaurid ornithopod (Dinosauria, Ornithischia) from the Late Jurassic of Portugal. *Journal of Vertebrate Paleontology*, **34**, 1102–1112.

Ezcurra, M. D. 2024. Exploring the effects of weighting against homoplasy in genealogies of palaeontological phylogenetic matrices. *Cladistics*, **40**, 242–281.

Ezcurra, M. D. and Agnolín, F. L. 2012. A new global palaeobiogeographical model for the late Mesozoic and early Tertiary. *Systematic Biology*, **61**, 553–566.

Fanti, F. 2012. Cretaceous continental bridges, insularity, and vicariance in the southern hemisphere: which route did dinosaurs take? 883–911. *In* Talent, J. A. (ed.) *Earth and life: Global biodiversity, extinction intervals and biogeographic perturbations through time*. Springer.

Fonseca, A. O., Reid, I. J., Venner, A., Duncan, R. J., Garcia, M. S. and Müller, R. T. 2024. A comprehensive phylogenetic analysis on early ornithischian evolution. *Journal of Systematic Palaeontology*, **22**, 2346577.

Foster, J. 2020. *Jurassic West: The dinosaurs of the Morrison formation and their world*, Second edition. Indiana University Press.

Galton, P. M. 2009. Notes on Neocomian (Lower Cretaceous) ornithopod dinosaurs from England – Hypsilophodon, Valdosaurus, "Camptosaurus", "Iguanodon" – and referred specimens from Romania and elsewhere. *Revue de Paléobiologie*, **28**, 64.

Galton, P. M. and Powell, H. P. 1980. The ornithischian dinosaur *Camptosaurus prestwichii* from the Upper Jurassic of England. *Palaeontology*, **23**, 411–443.

Gasca, J. M., Canudo, J. I., Ruiz-Omeñaca, J. I. and Moreno-Azanza, M. 2015. New material and phylogenetic position of the basal iguanodont dinosaur *Delapparentia turolensis* from the Barremian (Early Cretaceous) of Spain. *Journal of Iberian Geology*, **41**, 57–70.

Gasulla, J. M., Escaso, F., Narváez, I., Ortega, F. and Sanz, J. L. 2015. A new sail-backed styracosternan (Dinosauria: Ornithopoda) from the Early Cretaceous of Morella, Spain. *PLoS One*, **10**, e0144167.

Gasulla, J. M., Escaso, F., Narváez, I., Sanz, J. L. and Ortega, F. 2022. New *Iguanodon bernissartensis* axial Bones (Dinosauria, Ornithopoda) from the Early Cretaceous of Morella, Spain. *Diversity*, **14**, 63.

Gavryushkina, A., Welch, D., Stadler, T. and Drummond, A. J. 2014. Bayesian inference of sampled ancestor trees for epidemiology and fossil calibration. *PLoS Computational Biology*, **10**, e1003919.

Goloboff, P. A. and Morales, M. E. 2023. TNT version 1.6, with a graphical interface for MacOS and Linux, including new routines in parallel. *Cladistics*, **39**, 144–153.

Grigorescu, D. and Csiki, Z. 2006. Ontogenetic development of *Telmatosaurus transsylvanicus* (Ornitischia: Hadrosauria) from the Maastrichtian of the Haţeg Basin, Romania-evidence from the limb bones. *Hantkeniana*, **5**, 20–26.

Harrison, J. A. and Manning, E. M. 1983. Extreme carpal variability in *Teleoceras* (Rhinocerotidae, Mammalia). *Journal of Vertebrate Paleontology*, **3**, 58–64.

Herne, M. C., Nair, J. P., Evans, A. R. and Tait, A. M. 2019. New small-bodied ornithopods (Dinosauria, Neornithischia) from the Early Cretaceous Wonthaggi Formation (Strzelecki Group) of the Australian-Antarctic rift system, with revision of *Qantassaurus intrepidus* Rich and Vickers-Rich, 1999. *Journal of Paleontology*, **93**, 543–584.

Ho, S. Y. W., Duchêne, S. and Duchêne, D. 2015. Simulating and detecting autocorrelation of molecular evolutionary rates among lineages. *Molecular Ecology Resources*, **15**, 688–696.

Horner, J. R., Weishampel, D. B. and Forster, C. A. 2004. Hadrosauridae. 438–463. *In* Weishampel, D. B., Dodson, P. and Osmolska, H. (eds) *The Dinosauria*, Second edition. University of California Press.

Hulke, J. W. 1880. Iguanodon Prestwichii, a new species from the Kimmeridge Clay, distinguished from I. Mantelli of the Wealden Formation in the SE of England and Isle of Wight by differences in the shape of the vertebral centra, by fewer than five sacral vertebræ, by the simpler character of its toothserrature, &c., founded on numerous fossil remains lately discovered at Cumnor, near Oxford. *Quarterly Journal of the Geological Society*, **36**, 433–456.

Kirkland, J. I., Sertich, J. J. W. and Titus, A. L. 2025. Dinosaur biostratigraphy of the non-marine Cretaceous of Utah. *Geological Society, London, Special Publications*, **545**, SP545-2023–211.

Klein, H., Gierliński, G. D., Oukassou, M., Saber, H., Lallensack, J. N., Lagnaoui, A., Hminna, A. and Charrière, A. 2023. Theropod and ornithischian dinosaur track assemblages from Middle to ?Late Jurassic deposits of the Central High Atlas, Morocco. *Historical Biology*, **35**, 320–346.

Krause, D. W., Sertich, J. J., O'Connor, P. M., Curry Rogers, K. and Rogers, R. R. 2019. The Mesozoic biogeographic history of Gondwanan terrestrial vertebrates: insights from Madagascar's fossil record. *Annual Review of Earth and Planetary Sciences*, **47**, 519–553.

Läng, É. and Goussard, F. 2007. Redescription of the wrist and manus of ?*Bothriospondylus madagascariensis*: new data on carpus morphology in Sauropoda. *Geodiversitas*, **29**, 549–560.

Lee, M. S. Y., Cau, A., Naish, D. and Dyke, G. J. 2014. Morphological clocks in paleontology, and a mid-Cretaceous origin of crown Aves. *Systematic Biology*, **63**, 442–449.

Leidy, J. 1858. [On the bones of a huge herbivorous saurian near Haddonfield]. *Proceedings of the Academy of Natural Sciences of Philadelphia*, **10**, 215–218.

Lewis, P. O. 2001. A likelihood approach to estimating phylogeny from discrete morphological character data. *Systematic Biology*, **50**, 913–925.

Li, Y., Ruta, M. and Wills, M. A. 2020. Craniodental and postcranial characters of non-avian Dinosauria often imply different trees. *Systematic Biology*, **69**, 638–659.

Lloyd, G. T., Davis, K. E., Pisani, D., Tarver, J. E., Ruta, M., Sakamoto, M., Hone, D. W. E., Jennings, R. and Benton, M. J. 2008. Dinosaurs and the Cretaceous terrestrial revolution. *Proceedings of the Royal Society B*, **275**, 2483–2490.

Lockwood, J. A., Martill, D. M. and Maidment, S. C. 2021. A new hadrosauriform dinosaur from the Wessex Formation, Wealden Group (Early Cretaceous), of the Isle of Wight, southern England. *Journal of Systematic Palaeontology*, **19**, 847–888.

Lockwood, J. A. F., Martill, D. M. and Maidment, S. C. R. 2024. *Comptonatus chasei*, a new iguanodontian dinosaur from the Lower Cretaceous Wessex Formation of the Isle of Wight, southern England. *Journal of Systematic Palaeontology*, **22**, 2346573.

Lockwood, J. A. F., Martill, D. M. and Maidment, S. C. R. 2025. The origins of neural spine elongation in iguanodontian dinosaurs and the osteology of a new sail-back styracosternan (Dinosauria, Ornithischia) from the Lower Cretaceous Wealden Group of England. *Papers in Palaeontology*, **11**, e70034.

Longrich, N. R., Suberbiola, X. P., Pyron, R. A. and Jalil, N.-E. 2021. The first duckbill dinosaur (Hadrosauridae: Lambeosaurinae) from Africa and the role of oceanic dispersal in dinosaur biogeography. *Cretaceous Research*, **120**, 104678.

Madzia, D., Arbour, V. M., Boyd, C. A., Farke, A. A., Cruzado-Caballero, P. and Evans, D. C. 2021. The phylogenetic nomenclature of ornithischian dinosaurs. *PeerJ*, **9**, e12362.

Maidment, S. C. and Barrett, P. M. 2014. Osteological correlates for quadrupedality in ornithischian dinosaurs. *Acta Palaeontologica Polonica*, **59**, 53–70.

Maidment, S. C. R., Chapelle, K. E. J., Bonsor, J. A., Button, D. and Barrett, P. M. 2022. Osteology and Relationships of *Cumnoria prestwichii* (Ornithischia: Ornithopoda) from the Late Jurassic of Oxfordshire, UK. *Monographs of the Palaeontographical Society*, **176**, 1–55.

Maidment, S., Ouarhache, D., Butler, R. J., Boumir, K., Oussou, A., Ech-Charay, K., El Khanchoufi, A. and Barrett, P. M. 2025. The world's oldest cerapodan ornithischian dinosaur from the Middle Jurassic of Morocco. *Royal Society Open Science*, **12**, 241624.

Maidment, S. C. R., Butler, R. J., Brusatte, S. L., Meade, L. E., Augustin, F. J., Csiki-Sava, Z. and Ősi, A. 2026. A hidden diversity of ceratopsian dinosaurs in Late Cretaceous Europe. *Nature*, **651**, 397–403.

Marsh, O. C. 1881. Principal characters of American Jurassic dinosaurs, Part V. *American Journal of Science*, **s3-21**, 417–423.

Mateus, O. and Antunes, M. 2001. *Draconyx loureiroi*, a new Camptosauridae (Dinosauria, Ornithopoda) from the Late Jurassic of Lourinhã, Portugal. *Annales de Paléontologie*, **87**, 61–73.

Matzke, N. J. 2014. Model selection in historical biogeography reveals that founder-event Speciation Is a Crucial Process in Island Clades. *Systematic Biology*, **63**, 951–970.

Matzke, N. J. 2018. BioGeoBEARS: BioGeography with Bayesian (and likelihood) evolutionary analysis with R scripts. version 1.1.1 [dataset]. GitHub. https://github.com/nmatzke/BioGeoBEARS

McDonald, A. T. 2011. The taxonomy of species assigned to *Camptosaurus* (Dinosauria: Ornithopoda). *Zootaxa*, **2783**, 52–68.

McDonald, A. T. 2012. Phylogeny of basal iguanodonts (Dinosauria: Ornithischia): an update. *PLoS One*, **7**, e36745.

Medrano-Aguado, E., Parrilla-Bel, J., Gasca, J. M., Alonso, A. and Canudo, J. I. 2023. Ornithopod diversity in the Lower Cretaceous of Spain: new styracosternan remains from the Barremian of the Maestrazgo Basin (Teruel province, Spain). *Cretaceous Research*, **144**, 105458.

Muscioni, M., Chiarenza, A. A., Delfino, M., Fabbri, M., Milocco, K. and Fanti, F. 2023. *Acynodon adriaticus* from Villaggio del Pescatore (Campanian of Italy): Anatomical and chronostratigraphic integration improves phylogenetic resolution in Hylaeochampsidae (Eusuchia). *Cretaceous Research*, **151**, 105631.

Norman, D. B. 1986. On the anatomy of *Iguanodon atherfieldensis* (Ornithischia: Ornithopoda). *Bulletin de l'Institut royal des Sciences naturelles de Belgique*, **56**, 281–372.

Norman, D. B. 2004. Basal iguanodontia. 413–437. *In* Weishampel, D. B., Dodson, P. and Osmólska, H. (eds) *The Dinosauria*, Second edition. California University Press.

Norman, D. B. 2011. On the osteology of the lower Wealden (Valanginian) ornithopod *Barilium dawsoni* (Iguanodontia: Styracosterna). *Special Papers in Palaeontology*, **86**, 165–194.

Norman, D. B. 2012. Iguanodontian taxa (Dinosauria: Ornithischia) from the lower Cretaceous of England and Belgium. *In* Godefroit, P. (ed.) *Bernissart dinosaurs and Early Cretaceous terrestrial ecosystems*. Indiana University Press.

Norman, D. B. 2015. On the history, osteology, and systematic position of the Wealden (Hastings group) dinosaur *Hypselospinus fittoni* (Iguanodontia: Styracosterna). *Zoological Journal of the Linnean Society*, **173**, 92–189.

Olsen, P., Sha, J., Fang, Y., Chang, C., Whiteside, J. H., Kinney, S., Sues, H.-D., Kent, D., Schaller, M. and Vajda, V. 2022. Arctic ice and the ecological rise of the dinosaurs. *Science Advances*, **8**, eabo6342.

Oussou, A., Falkingham, P. L., Butler, R. J., Boumir, K., Ouarhache, D., Ech-Charay, K., Charrière, A. and Maidment, S. C. R. 2023. New Middle to ?Late Jurassic dinosaur tracksites in the Central High Atlas Mountains, Morocco. *Royal Society Open Science*, **10**, 231091.

Owen, R. 1842. Report on British fossil reptiles. Part II. *Report of the Eleventh Meeting of the British Association for the Advancement of Science*, **1842**, 60–204.

Panciroli, E., Funston, G. F., Maidment, S. C. R., Butler, R. J., Benson, R. B. J., Crawford, B. L., Fair, M., Fraser, N. C. and Walsh, S. 2025. The first and most complete dinosaur skeleton from the Middle Jurassic of Scotland. *Earth and Environmental Science Transactions of the Royal Society of Edinburgh*, 1–12. https://doi.org/10.1017/S1755691024000148

Pol, D., Ramezani, J., Gomez, K., Carballido, J. L., Carabajal, A. P., Rauhut, O. W. M., Escapa, I. H. and Cúneo, N. R. 2020. Extinction of herbivorous dinosaurs linked to Early Jurassic global warming event. *Proceedings of the Royal Society B*, **287**, 20202310.

Poole, K. 2022. Phylogeny of iguanodontian dinosaurs and the evolution of quadrupedality. *Palaeontologia Electronica*, **25** (3), a30.

Prieto-Márquez, A., Fondevilla, V., Sellés, A. G., Wagner, J. R. and Galobart, À. 2019. *Adynomosaurus arcanus*, a new lambeosaurine dinosaur from the Late Cretaceous Ibero-Armorican Island of the European archipelago. *Cretaceous Research*, **96**, 19–37.

Rambaut, A., Drummond, A. J., Xie, D., Baele, G. and Suchard, M. A. 2018. Posterior summarization in Bayesian phylogenetics using Tracer 1.7. *Systematic Biology*, **67**, 901–904.

Randazzo, V., Di Stefano, P., Schlagintweit, F., Todaro, S., Cacciatore, M. S. and Zarcone, G. 2021. The migration path of Gondwanian dinosaurs toward Adria: New insights from the Cretaceous of NW Sicily (Italy). *Cretaceous Research*, **126**, 104919.

Rauhut, O. W. and Pol, D. 2019. Probable basal allosauroid from the early Middle Jurassic Cañadón Asfalto Formation of Argentina highlights phylogenetic uncertainty in tetanuran theropod dinosaurs. *Scientific Reports*, **9**, 18826.

Rauhut, O. W. M., Carballido, J. L. and Pol, D. 2015. A diplodocid sauropod dinosaur from the Late Jurassic Cañadón Calcáreo Formation of Chubut, Argentina. *Journal of Vertebrate Paleontology*, **35**, e982798.

Rauhut, O. W., Huebner, T. R. and Lanser, K.-P. 2016. A new megalosaurid theropod dinosaur from the late Middle Jurassic

(Callovian) of north-western Germany: implications for theropod evolution and faunal turnover in the Jurassic. *Palaeontologia Electronica*, **19** (2), 26A.

Ronquist, F. 1997. Dispersal-vicariance analysis: a new approach to the quantification of historical biogeography. *Systematic Biology*, **46**, 195–203.

Ronquist, F., Klopfstein, S., Vilhelmsen, L., Schulmeister, S., Murray, D. L. and Rasnitsyn, A. P. 2012a. A total-evidence approach to dating with fossils, applied to the early radiation of the Hymenoptera. *Systematic Biology*, **61**, 973–999.

Ronquist, F., Teslenko, M., Van Der Mark, P., Ayres, D. L., Darling, A., Höhna, S., Larget, B., Liu, L., Suchard, M. A. and Huelsenbeck, J. P. 2012b. MrBayes 3.2: efficient Bayesian phylogenetic inference and model choice across a large model space. *Systematic Biology*, **61**, 539–542.

Rotatori, F. M., Chiarenza, A. A., Fanti, F. and Moreno-Azanza, M. 2026. The early origin of Iguanodontia: new insights on the macroevolution, diversity and biogeography of the clade [dataset]. MorphoBank, P5992. https://www.morphobank.org/permalink/?P5992

Rotatori, F. M., Escaso, F., Camilo, B., Bertozzo, F., Malafaia, E., Mateus, O., Mocho, P., Ortega, F. and Moreno-Azanza, M. 2025. Evidence of large-sized ankylopollexian dinosaurs (Ornithischia: Iguanodontia) in the Upper Jurassic of Portugal. *Journal of Systematic Palaeontology*, **23**, 2470789.

Rotatori, F. M., Ferrari, L., Sequero, C., Camilo, B., Mateus, O. and Moreno-Azanza, M. 2023. An unexpected early-diverging iguanodontian dinosaur (Ornithischia, Ornithopoda) from the Upper Jurassic of Portugal. *Journal of Vertebrate Paleontology*, **43**, e2310066.

Rotatori, F. M., Moreno-Azanza, M. and Mateus, O. 2020. New information on ornithopod dinosaurs from the Late Jurassic of Portugal. *Acta Palaeontologica Polonica*, **65**, 35–57.

Rotatori, F. M., Moreno-Azanza, M. and Mateus, O. 2022. Reappraisal and new material of the holotype of *Draconyx loureiroi* (Ornithischia: Iguanodontia) provide insights on the tempo and modo of evolution of thumb-spiked dinosaurs. *Zoological Journal of the Linnean Society*, **195**, 125–156.

Rozadilla, S., Agnolín, F. L. and Novas, F. E. 2019. Osteology of the Patagonian ornithopod *Talenkauen santacrucensis* (Dinosauria, Ornithischia). *Journal of Systematic Palaeontology*, **17**, 2043–2089.

Rozadilla, S., Cruzado-Caballero, P. and Calvo, J. O. 2020. Osteology of Ornithopod *Macrogryphosaurus gondwanicus* (Dinosauria, Ornithischia) from the Upper Cretaceous of Patagonia, Argentina. *Cretaceous Research*, **108**, 104311.

Ruebsam, W. and Al-Husseini, M. 2020. Calibrating the Early Toarcian (Early Jurassic) with stratigraphic black holes (SBH). *Gondwana Research*, **82**, 317–336.

Ruhl, M., Hesselbo, S. P., Hinnov, L., Jenkyns, H. C., Xu, W., Riding, J. B., Storm, M., Minisini, D., Ullmann, C. V. and Leng, M. J. 2016. Astronomical constraints on the duration of the Early Jurassic Pliensbachian Stage and global climatic fluctuations. *Earth and Planetary Science Letters*, **455**, 149–165.

Ruiz-Omeñaca, J. I. 2011. *Delapparentia turolensis* nov. gen et sp., un nuevo dinosaurio iguanodontoideo (Ornithischia: Ornithopoda) en el Cretácico Inferior de Galve. *Estudios Geológicos*, **67**, 83–110.

Ruiz-Omeñaca, J. I., Pereda Suberbiola, X. and Galton, P. M. 2006. *Callovosaurus leedsi*, the earliest dryosaurid dinosaur (Ornithischia: Euornithopoda) from the Middle Jurassic of England. 3–16. *In* Carpenter, K. (ed.) *Horns and beaks: Ceratopsian and ornithopod dinosaurs*. Indiana University Press.

Sánchez-Fenollosa, S., Verdú, F. J. and Cobos, A. 2023. The largest ornithopod (Dinosauria: Ornithischia) from the Upper Jurassic of Europe sheds light on the evolutionary history of basal ankylopollexians. *Zoological Journal of the Linnean Society*, **199**, 1013–1033.

Santos-Cubedo, A., De Santisteban, C., Poza, B. and Meseguer, S. 2021. A new styracosternan hadrosauroid (Dinosauria: Ornithischia) from the Early Cretaceous of Portell, Spain. *PLoS One*, **16**, e0253599.

Schöllhorn, I., Adatte, T., van de Schootbrugge, B., Houben, A., Charbonnier, G., Janssen, N. and Föllmi, K. B. 2020. Climate and environmental response to the break-up of Pangea during the Early Jurassic (Hettangian-Pliensbachian); the Dorset coast (UK) revisited. *Global and Planetary Change*, **185**, 103096.

Seeley, H. G. 1888a. On Cumnoria, an iguanodont genus founded upon the Iguanodon prestwichi, Hulke. *Report of the British Association of the Advancement of Science*, **57**, 698.

Seeley, H. G. 1888b. I. On the classification of the fossil animals commonly named Dinosauria. *Proceedings of the Royal Society of London*, **43**, 165–171.

Sereno, P. C. 1986. Phylogeny of the bird-hipped dinosaurs (Order Ornithischia). *National Geographic Research*, **2**, 234–256.

Silva, R. L. and Duarte, L. V. 2015. Organic matter production and preservation in the Lusitanian Basin (Portugal) and Pliensbachian climatic hot snaps. *Global and Planetary Change*, **131**, 24–34.

Silva, R. L., Duarte, L. V., Wach, G. D., Ruhl, M., Sadki, D., Gómez, J. J., Hesselbo, S. P., Xu, W., O'Connor, D., Rodrigues, B. and Filho, J. G. M. 2021. An Early Jurassic (Sinemurian–Toarcian) stratigraphic framework for the occurrence of organic matter preservation intervals (OMPIs). *Earth-Science Reviews*, **221**, 103780.

Simões, T. R., Caldwell, M. W. and Pierce, S. E. 2020a. Sphenodontian phylogeny and the impact of model choice in Bayesian morphological clock estimates of divergence times and evolutionary rates. *BMC Biology*, **18**, 1–30.

Simões, T. R., Vernygora, O., Caldwell, M. W. and Pierce, S. E. 2020b. Megaevolutionary dynamics and the timing of evolutionary innovation in reptiles. *Nature Communications*, **11**, 3322.

Stubbs, T. L., Benton, M. J., Elsler, A. and Prieto-Márquez, A. 2019. Morphological innovation and the evolution of hadrosaurid dinosaurs. *Paleobiology*, **45**, 347–362.

Sugiura, N. 1978. Further analysis of the data by Akaike's information criterion and the finite corrections: further analysis of the data by Akaike's. *Communications in Statistics – Theory and Methods*, **7**, 13–26.

Takasaki, R., Fiorillo, A. R., Tykoski, R. S. and Kobayashi, Y. 2020. Re-examination of the cranial osteology of the Arctic Alaskan hadrosaurine with implications for its taxonomic status. *PLoS One*, **15**, e0232410.

Taquet, P. 1976. *Géologie et paléontologie du gisement de Gadoufaoua (Aptien du Niger) [Geology and paleontology of the Gadoufaoua locality (Aptian of Niger)]*. Centre National de la Recherche Scientifique, Paris, Cahiers de Paléontologie, 191 pp.

Taquet, P. and Russell, D. A. 1999. A massively-constructed iguanodont from Gadoufaoua, Lower Cretaceous of Niger. *Annales de Paléontologie*, **85**, 85–96.

Thierry, J. 2000. Middle Toarcian (180–178 Ma). 60–70. *In* Crasquin, S. (ed.) *Atlas Peri-Tethys palaeogeographical maps*. CCGM/CGMW, Paris.

Tsogtbaatar, K., Weishampel, D. B., Evans, D. C. and Watabe, M. 2019. A new hadrosauroid (Dinosauria: Ornithopoda) from the Late Cretaceous Baynshire Formation of the Gobi Desert (Mongolia). *PLoS One*, **14**, e0208480.

Tucker, R. T., Crowley, J. L., Mohr, M. T., Renaut, R. K., Makovicky, P. J. and Zanno, L. E. 2023. Exceptional age constraint on a fossiliferous sedimentary succession preceding the Cretaceous Thermal Maximum. *Geology*, **51**, 962–967.

Upchurch, P. and Chiarenza, A. A. 2024. A brief review of non-avian dinosaur biogeography: state-of-the-art and prospectus. *Biology Letters*, **20**, 20240429.

Verdú, F. J., Godefroit, P., Royo-Torres, R., Cobos, A. and Alcalá, L. 2017b. Individual variation in the postcranial skeleton of the Early Cretaceous *Iguanodon bernissartensis* (Dinosauria: Ornithopoda). *Cretaceous Research*, **74**, 65–86.

Verdú, F. J., Royo-Torres, R., Cobos, A. and Alcala, L. 2015. Perinates of a new species of Iguanodon (Ornithischia: Ornithopoda) from the lower Barremian of Galve (Teruel, Spain). *Cretaceous Research*, **56**, 250–264.

Verdú, F. J., Royo-Torres, R., Cobos, A. and Alcalá, L. 2017a. New systematic and phylogenetic data about the early Barremian *Iguanodon galvensis* (Ornithopoda: Iguanodontoidea) from Spain. *Historical Biology*, **30**, 437–474.

Vidarte, C. F., Calvo, M. M., Fuentes, F. M. and FuenteS, M. M. 2016. Un nuevo dinosaurio estiracosterno (Ornithopoda: Ankylopollexia) del Cretácico Inferior de España. *Spanish Journal of Palaeontology*, **31**, 407–446.

Vila, B., Sellés, A., Moreno-Azanza, M., Razzolini, N. L., Gil-Delgado, A., Canudo, J. I. and Galobart, À. 2022. A titanosaurian sauropod with Gondwanan affinities in the latest Cretaceous of Europe. *Nature Ecology & Evolution*, **6**, 288–296.

Weishampel, D. B., Jianu, C.-M., Csiki, Z. and Norman, D. B. 2003. Osteology and phylogeny of *Zalmoxes* (ng), an unusual euornithopod dinosaur from the latest Cretaceous of Romania. *Journal of Systematic Palaeontology*, **1**, 65–123.

Wignall, P. B. 2001. Large igneous provinces and mass extinctions. *Earth-Science Reviews*, **53**, 1–33.

Xu, X., Tan, Q., Gao, Y., Bao, Z., Yin, Z., Guo, B., Wang, J., Tan, L., Zhang, Y. and Xing, H. 2018. A large-sized basal ankylopollexian from East Asia, shedding light on early biogeographic history of Iguanodontia. *Science Bulletin*, **63**, 556–563.

Zanno, L. E., Gates, T. A., Avrahami, H. M., Tucker, R. T. and Makovicky, P. J. 2023. An early-diverging iguanodontian (Dinosauria: Rhabdodontomorpha) from the Late Cretaceous of North America. *PLoS One*, **18**, e0286042.

Zanno, L. E., Tucker, R. T., Canoville, A., Avrahami, H. M., Gates, T. A. and Makovicky, P. J. 2019. Diminutive fleet-footed tyrannosauroid narrows the 70-million-year gap in the North American fossil record. *Communications Biology*, **2**, 64.

Zhang, C. 2022. Selecting and averaging relaxed clock models in Bayesian tip dating of Mesozoic birds. *Paleobiology*, **48**, 340–352.